AD_____

GRANT NUMBER DAMD17-94-J-4235

TITLE: Diagnostic Imaging/Mammography Certification and Quantitative Evaluation of Ultrasound CT Breast Imaging System

PRINCIPAL INVESTIGATOR: Helmar S. Janée
Michael P. André, Ph.D.

CONTRACTING ORGANIZATION: University of California, San Diego
La Jolla, California 92093

REPORT DATE: July 1996

TYPE OF REPORT: Final

PREPARED FOR: Commander
U.S. Army Medical Research and Materiel Command
Fort Detrick, Frederick, Maryland 21702-5012

REPORT DOCUMENTATION PAGE

Form Approved
OMB No. 0704-0188

1. AGENCY USE ONLY *(Leave blank)*	2. REPORT DATE	3. REPORT TYPE AND DATES COVERED
	July 1996	Final 1 Jul 94 - 30 Jun 96)

4. TITLE AND SUBTITLE
Diagnostic Imaging/Mammography Certification and Quantitative Evaluation of Ultrasound CT Breast Imaging System

5. FUNDING NUMBERS
DAMD17-94-J-4235

6. AUTHOR(S)
Helmar S. Janée
Michael P. André, Ph.D.

7. PERFORMING ORGANIZATION NAME(S) AND ADDRESS(ES)
University of California, San Diego
La Jolla, California 92093

8. PERFORMING ORGANIZATION REPORT NUMBER

9. SPONSORING/MONITORING AGENCY NAME(S) AND ADDRESS(ES)
Commander
U.S. Army Medical Research and Materiel Command
Fort Detrick, Frederick, Maryland 2170-25012

10. SPONSORING/MONITORING AGENCY REPORT NUMBER

11. SUPPLEMENTARY NOTES

12a. DISTRIBUTION / AVAILABILITY STATEMENT
Approved for public release; distribution unlimited

12b. DISTRIBUTION CODE

13. ABSTRACT *(Maximum 200 words)*

This report summarizes activity in the two principal areas: 1) Preparation for Diagnostic Imaging/ Mammography Certification and 2) Dissertation research on Breast Imaging using Ultrasound Diffraction Tomography techniques. The first task included completion of clinical rotation courses in X-ray radiography and CT, Nuclear Medicine, MRI, and Ultrasound Imaging at the UCI Radiological Sciences Department. A M.S. degree in Radiological Sciences was granted in March, 1995. Quality assurance of diagnostic imaging equipment including mammography systems and radiation shielding evaluations were carried out at several institutions. Dissertation research focused on the performance of two ultrasound diffraction tomography systems developed for breast imaging. Measurements of the frequency-dependent MTF of a 1 MHz transducer ring were completed. Speed of sound linearity in the absence of aberrating media was established for both rings over a nominally ± 10% range. These data have been interpreted to characterize the validity of the first order Born approximation in inverse scattering problems. Ultrasound scatter data from clinical trials on human breast tissue have been analyzed in terms of stastistical distribution functions to characterize breast tissue. Tomographic breast images from eight patients have been evaluated in order to establish quantitative tissue contrast values for both normal and pathological breast tissue

14. SUBJECT TERMS	15. NUMBER OF PAGES
Breast Cancer	47
	16. PRICE CODE

17. SECURITY CLASSIFICATION OF REPORT	18. SECURITY CLASSIFICATION OF THIS PAGE	19. SECURITY CLASSIFICATION OF ABSTRACT	20. LIMITATION OF ABSTRACT
Unclassified	Unclassified	Unclassified	Unlimited

FOREWORD

Opinions, interpretations, conclusions and recommendations are those of the author and are not necessarily endorsed by the US Army.

____ Where copyrighted material is quoted, permission has been obtained to use such material.

____ Where material from documents designated for limited distribution is quoted, permission has been obtained to use the material.

__/__ Citations of commercial organizations and trade names in this report do not constitute an official Department of Army endorsement or approval of the products or services of these organizations.

____ In conducting research using animals, the investigator(s) adhered to the "Guide for the Care and Use of Laboratory Animals," prepared by the Committee on Care and Use of Laboratory Animals of the Institute of Laboratory Resources, National Research Council (NIH Publication No. 86-23, Revised 1985).

____ For the protection of human subjects, the investigator(s) adhered to policies of applicable Federal Law 45 CFR 46.

____ In conducting research utilizing recombinant DNA technology, the investigator(s) adhered to current guidelines promulgated by the National Institutes of Health.

____ In the conduct of research utilizing recombinant DNA, the investigator(s) adhered to the NIH Guidelines for Research Involving Recombinant DNA Molecules.

____ In the conduct of research involving hazardous organisms, the investigator(s) adhered to the CDC-NIH Guide for Biosafety in Microbiological and Biomedical Laboratories.

Edward L. Alecci 7/30/96

PI - Signature Date

TABLE OF CONTENTS

INTRODUCTION

Problem Statement

This fellowship addresses two important steps in the battle against breast cancer: earlier detection through improvements in diagnostic techniques and improved quality control through training of qualified personnel, specifically diagnostic radiology physicists. The severity of the impact of mammary carcinoma on the health and mortality of US women has been described extensively in the literature. [1-4] Many approaches to the improvement in the overall treatment of the problem have been proposed and are being pursued. Among approaches to address this problem is research in improved breast imaging techniques for earlier detection. The latter stresses the need for the general availability of safe and low-cost diagnostic techniques to monitor the population at risk. This is particularly urgent in view of the fact that the persistent mortality rate despite improvements in diagnosis and treatment is in part explained by the fact that minority, older and low-income women have restricted access to mammography.[4] While conventional mammography is quite effective as a screening tool for the detection of microcalcifications, early detection of breast cancer is frequently complicated by the occurrence of benign fibrocystic changes.[5,6] These changes include cyst formation, calcium and cholesterol precipitation, lobular secretion and epithelial hyperplasia and are normal variations of breast tissue growth. The formation of these benign lesions most commonly occurs in the fatty tissue which surrounds the glandular tissue and these lesions generally have smooth, circumscribed borders. This normal dynamic evolution of the breast increases the probability of incorrect diagnosis of early mammary carcinoma.

Background

The accreditation of medical physicists in Diagnostic Imaging Physics and Mammography by professional organizations such as the American Association of Physicists in Medicine (AAPM)[7], the American College of Radiology (ACR)[8], the Federal Drug Administration (FDA) or the State of California (Dept. of Health Services) has general education as well as experience requirements. The former were addressed through graduate studies in the Department of Radiological Sciences at the University of California, Irvine, and through participation in specific professional training courses. Work experience requirements were principally met through my work as medical physicist in the University of California, San Diego, Department of Radiology and my woc (work without compensation) association with the Veterans Affairs Medical Center in La Jolla, CA.

The standard for diagnostic breast imaging has evolved over many years to be X-ray mammography. It has superb resolution and clarity for detection of clusters of microcalcifications and for identification of lesion borders. However, early carcinoma is often difficult to distinguish from benign fibrocystic changes and this leads to a high number of false positive diagnoses and thus unnecessary biopsies.[9,10] There has been extensive research to provide adjunctive or alternative imaging systems to mammography including digital x-ray imaging, magnetic resonance imaging (MRI) and ultrasound sonography. In the early 1980's, dedicated ultrasound scanners were

evaluated for whole breast imaging.[11-14]. Today, the role of ultrasound in breast imaging is primarily limited to evaluating the composition of larger lesions detected by mammography in terms of cystic (benign) versus solid (benign or malignant).[11]

Computed tomography (CT) is a powerful and routine technique in x-ray, nuclear medicine and magnetic resonance imaging. In the 1970's and early 1980's, several investigators sought with limited success to apply these image reconstruction methods to pulse-transmission ultrasound of breast tissue.[12-17] The goal of these methods was to improve differentiation of breast cancer from numerous benign conditions of the breast by measuring several acoustic properties of the lesion. A particularly interesting approach to ultrasound CT is diffraction tomography which has received substantial theoretical treatment and holds the potential to account for the inherent diffraction in sound propagation. Despite considerable theoretical development of diffraction tomography, laboratory implementation has been limited and has met with variable success.[18-20]

The work which constitutes the dissertation research portion of this fellowship is based on a new approach to ultrasound diffraction tomography which is largely the result of a collaboration between researchers at UCSD and Thermotrex Technologies Corporation (TTC).[21-25] This approach is described briefly in a subsequent section (Methods).

Purpose

Certification of medical physicists in Diagnostic Radiological Physics and Mammography permits them to assure and verify the proper and safe performance of diagnostic imaging equipment and thus protects the safety of the patients. Additionally, maintenance of imaging performance standards results in improved and more accurate diagnostics and thus serves the general patient population. This is particularly critical in mammography where the imaging procedures have to be optimized to permit earliest detection of breast cancers. This has recently been recognized by the establishment of more stringent standards both for the certification of medical physicists and the performance of mammography centers. Thorough training in diagnostic imaging physics and mammography for medical physicists thus proves to be a benefit to the local community in that the skills and training acquired will serve the general population at risk, as well as older, minority and poor women who presently receive inadequate diagnostic screening for breast cancer.

The principal purpose in the development of the ultrasound CT scanner by the UCSD/TTC team was that the differences described above between this new approach and previous efforts to construct a practical ultrasound CT (USCT) system might prove to be advantageous. The principal advantages were: 1) Low-frequency, continuous-wave insonification; 2) large number of projections around the whole object; 3) high speed sampling at optimal spatial frequency; 4) large field of view. A laboratory prototype, described in the Methods section, suggested that the approach may have utility as an adjunctive tool to mammography. The human-sized device which was developed produces unique images of a very large eight-inch field of view in a coronal format. In cases where an x-ray mammogram reveals a suspicious lesion, monitoring with USCT could provide a non-invasive alternative to biopsy.

The focus of the dissertation research is the quantitative description of the imaging

characteristics of this new ultrasound computed tomography procedure. Diffraction tomography potentially affords the characterization of certain breast tissue properties such as speed of sound, density, attenuation and compressibility. Before a quantitative interpretation of such parameters can be realized, however, the system needs to be calibrated with phantoms that establish the linearity, resolution and dynamic range of the reconstructed images. This is particularly essential in the development of a clinical breast imaging system since breast tissue is complex, the breast has few recognizable anatomical landmarks and thus imaging artifacts, noise and aberrations must be carefully characterized and, if possible, eliminated, in order to reduce the probability of mis-diagnosis or misinterpretation of the images.

Methods

The emphasis of this pre-doctoral fellowship is on two areas that are related in subject matter but rather distinct in terms of the activities and approaches involved. The first task addresses preparation for board certification in Diagnostic Radiological Physics and Mammography and thus contains both formal and on-the-job training elements. Certification in diagnostic radiological physics requires both formal training leading to a graduate degree in physics, medical physics or a related subject area as well as documented work-experience in the field under the supervision of certified medical physicists. This report describes the training, work experience and degree(s) conferred during the first year of this fellowship. The second task involves dissertation research on a full-breast imaging technique based on ultrasound diffraction tomography principles realized in a recently developed scanning system.

1. Certification/Diagnostic Radiological Physics and Mammography

The AAPM Report on the Clinical Training of Radiological Physicists[7] defines the areas of activity of the Diagnostic Radiological Physicist as follows: 1) Calibration of imaging equipment; 2) Calculation and measurement of exposure and dose; 3) Improving and maintaining medical image quality; 4) Training of physicists, clinical diagnostic imaging residents, radiological and ultrasound technologists, and other allied health professionals in diagnostic radiology; 5) Education of health professionals and the public in diagnostic imaging physics and radiation effects; 6) Additional duties such as developmental studies, administrative duties and research.

Competence in the above radiological and clinical areas derives from fundamental understanding of and facility with radiation physics, general and specific imaging concepts, radiation biology and basic clinical concepts including anatomy, physiology and patient procedures.

Effective January 1, 1993, The American College of Radiology (ACR) has established qualification requirements for accreditation of medical physicists in mammography under the Mammography Quality Standards Act (MQSA). These specify that for eligibility, one of two sets of criteria must be met:

1) Medical physicist certified in Diagnostic Radiological Physics or Radiological Physics by any certifying body recognized by the American College of Radiology.

2) Until January 1, 1996, alternative criteria will be recognized.

a) M.S. or M.A. degree in physics, applied physics, radiological physics, biophysics, health physics engineering, public health when B.S. is in a physical science.

b) Training in biological sciences.

c) Minimum 1 year training in medical physics in the area of diagnostic radiological physics.

d) Minimum 2 years experience conducting mammography equipment performance evaluations.

Additionally, it is specified that a candidate satisfying either of the above requirements have had at least fifteen (15) hours of documented continuing medical education training in mammography physics within the last three years.

2. Dissertation Research

The focus of the doctoral dissertation is the quantitative description of the imaging characteristics of a new ultrasound computed tomography procedure that is intended to serve as an adjunct to conventional x-ray mammography. This new approach is based on two human-size systems designed specifically for breast imaging that use low-frequency (0.2-1.4 MHz) continuous-wave sound , cylindrical arrays of 1024 and 512 transducers, high spatial frequency sampling of the wavefront and a unique diffraction tomographic reconstruction method.

This method of ultrasound CT employs a full circle of transducers which surrounds and defines the field of view (Figure 1). The object is coupled to the transducer array by a water bath. One element at a time transmits a continuous single-frequency sound beam with a cylindrical wavefront. The system reaches steady state in about 300 μsec, at which point the remaining transducers record amplitude and phase (relative to the transmitter) of the signal scattered the object to be imaged . Each transducer is activated as a transmitter in turn, sequentially probing along a complete 360^{o} arc.

The laboratory systems were constructed to test feasibility of the method for breast imaging. The 1 MHz SCT device shown in Figure 2 consists of 1024 lead zirconate titanate (PZT) transducers, arranged in an eight-inch cylinder. The breast imaging system, shown in Figure 3, consists of a control console which contains all the signal generation and data acquisition and processing electronics and computers and a couch on which the patient reclines with the breast suspended in a water tank incorporating the transducer array. The tank can be raised and lowered for slice selection and moved laterally for optimum patient positioning.

The emphasis of the first year's work was on evaluating the acoustical characteristics of the two transducer rings, on establishing initial system performance figures of merit, on assessing the effects of various object and data acquisition variables on image quality and on participating in a clinical trials series. These tasks followed the plan in the Statement of Work of the original proposal. An additional task was introduced in the first year and expanded in the second: analysis of the raw signals scattered by breast tissue. This work is based on similar statistical analyses reported by Steinberg and co-workers as well as other investigators[26-35] who have studied the amplitude and phase distortions of the wavefront of the insonifying beam when passing through tissue and frequently breast tissue. The relevance of this sort of data analysis is that it describes and summarizes the strength of the scattering of the ultrasound beam and thus

was felt to be potentially an indicator of the suitability or lack thereof of certain reconstruction algorithms based on linearizing assumptions such as the Born approximation. A brief discussion is presented of a new operator-based formalism that suggests that the Born and Rytov approximations represent extreme endpoints of a continuos reconstruction formalism. Due to limited access to the imaging system as a result of equipment problems in the second year, a second new task was added, the analysis of breast tissue contrast for patient data available from clinical trials conducted at the UCSD Center for Women's Health. Both normal tissue and tissue diagnosed with pathology on the basis of conventional mammography were evaluated.

The next section contains a description of the work performed during the fellowship and examples of some of the results obtained, as well as discussions of the experimental and analysis techniques employed. The tasks addressed are summarized below:

- Characterization of the transmit beam patterns and slice profiles of both the 1 MHz and 0.5 MHz SCT rings.

- MTF (Modulation Transfer Function) measurements vs. frequency and position within the measurement tank for the 1 MHz SCT ring.

- Speed of Sound contrast linearity for various size objects in a non-aberrating medium (water) for both 1 MHz and 0.5 MHz SCT rings determined with several reconstruction algorithms.

- Studies of *in vivo* scattering amplitude distribution of breast tissue from patients scanned during the clinical trials phase.

- Exploration of a new operator-based formalism for the Born and Rytov approximations.

- Breast tissue contrast and texture analysis from clinical patient data obtained at the UCSD Center for Women's Health.

- Presentation of papers at the AAPM Annual Meetings in Anaheim, CA in July, 1994, and Philadelphia in July, 1996; at the American Institute of Ultrasound in Medicine Conference in San Francisco, CA in March, 1995, and at the 22nd International Acoustical Imaging Conference, Florence, Italy, Sept. 1995.

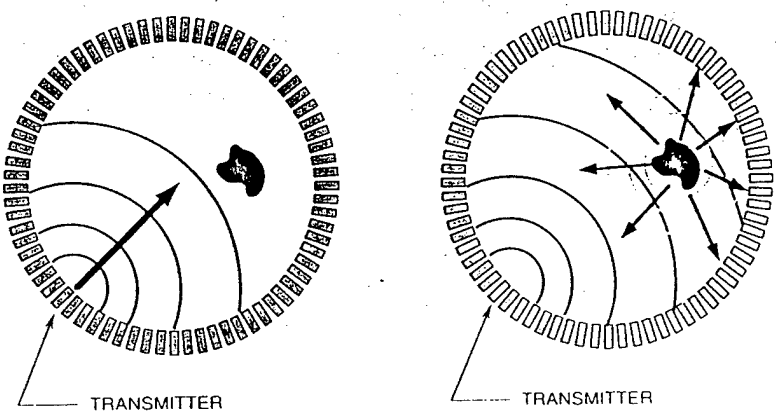

Figure 1. Scanning Geometry of Ultrasound Diffraction Tomography Breast Imaging System.

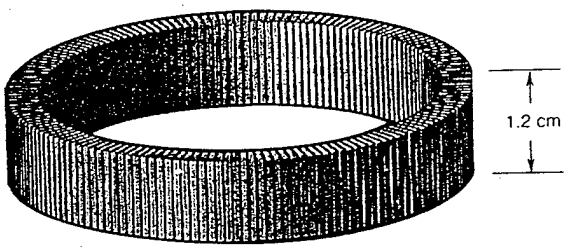

- 1024 transducers, 20 cm bore
- Operating frequency,700 kHz - 1.2 MHz
- 0.37 mm image resolution
- Data acquisition time, 0.5 sec
- Image reconstruction time, 2 minutes

93-16492

Figure 2. 1024-element 1 MHz SCT Transducer Ring.

TTC CLINICAL TEST UNIT LORAD

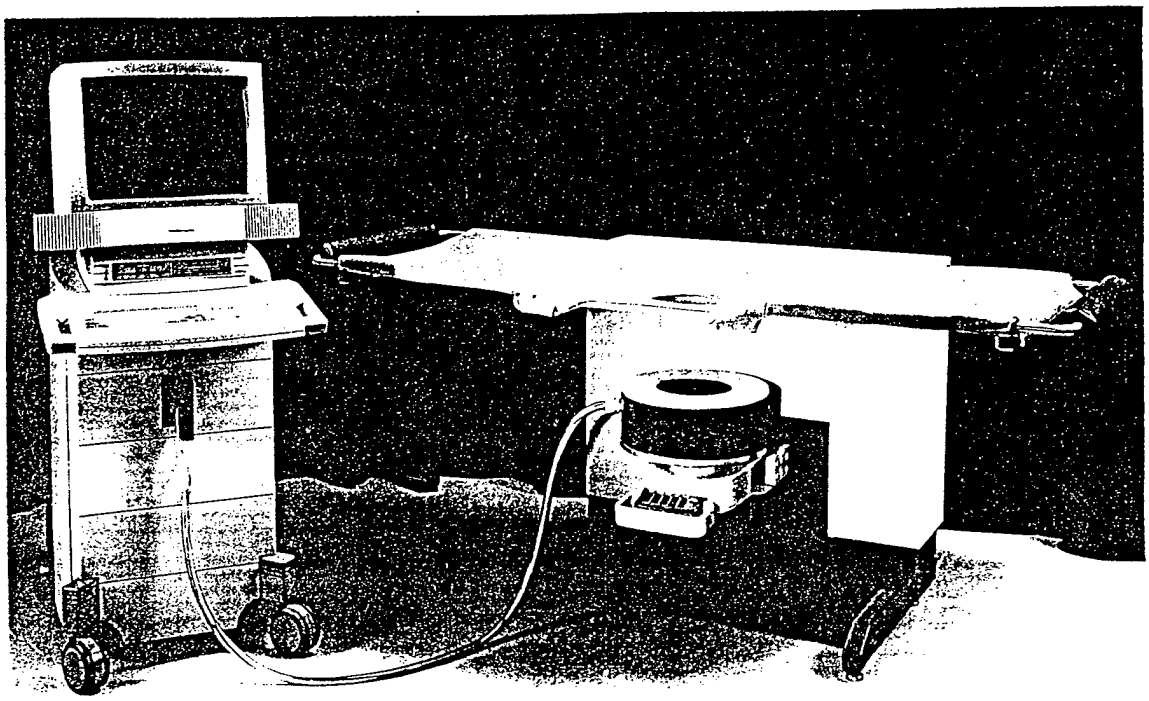

Figure 3. TTC/LORAD SCT Clinical Test Unit

BODY

The main accomplishments of the pre-doctoral fellowship in both the training and dissertation research areas are described in this section. Results of the research on the performance evaluations of an ultrasound diffraction tomography breast imaging system and of some early clinical patient data are summarized The thrust of this report is not only to present final results and conclusions about the technology issues raised in the proposal for this work, but to indicate progress made and to point out areas which are new or which differ significantly from the statement of work.

I. Certification in Diagnostic Radiological Physics, Mammography

Below are summarized the training activities, formal education elements and practical work experience that all satisfy various requirements for board certification in Diagnostic Radiological Physics and in Mammography by agencies such as the American Association of Physicists in Medicine(AAPM), the American College of Radiology (ACR), the American College of Medical Physics (ACMP), the State of California (Dept. of Health Services) and the Federal Drug Administration (FDA).

1.1 Formal Education

Course Work--Three academic quarters of Clinical Rotation in several areas addressing various imaging modalities were completed in the Radiological Sciences Department of the University of California, Irvine, CA (UCI). These courses were conducted mostly at the UCI Medical Center in Orange, CA but also included visits to imaging centers such as the UCI Brain Imaging Center. These rotations emphasized observation of and participation in daily, routine activities in a hospital setting that related to the operation, quality control and interpretation of various imaging systems. The rotations were as follows:

- **X-Ray Radiography/Fluoroscopy**--Participation in system quality control activities, acquisition of images, review of x-rays with radiologists.

- **X-Ray CT**--Calibration of a CT Scanner using a Calphan phantom, measurements of system resolution, contrast sensitivity, slice thickness, linearity. Observation of patient scans and review of tomographic images with radiologists.

- **MRI**--Clinical applications presentation by radiologists, observation of patient scans, review of patient images with radiologists, daily and weekly system calibration procedures using several phantoms.

- **Mammography/Ultrasound**--Participation with sonographers on patient scans, evaluation of mammograms and adjunctive ultrasound scans of a range of breast types and pathologies with radiologists, daily ultrasound and mammography systems checks and calibrations.

- **Radiation Oncology**--Review if linac calibration procedures, generation of patient depth-dose profiles from bremsstrahlung and electron beam irradiation, attendance of weekly tumor review boards, review of treatment planning procedures and participation in patient treatments.

- **Nuclear Medicine**--Presentation of and participation in radiopharmaceuticals preparation and assaying, observation of gamma camera patient imaging, daily camera calibration procedures, review with radiologists of SPECT images, review of PET procedures including cyclotron operation for radiopharmaceutical production, observation of patient treatment and imaging, review of images with radiologists.

- **Digital Angiography**--Review of digital fluoroscopy procedures, participation in system performance calibrations, implementation of various digital subtraction techniques.

Degrees Conferred: M.S. degree in Radiological Sciences, March, 1995. University of California, Irvine, CA.

Doctoral Dissertation: "The Empirical Determination of the Range of Validity of the Born Approximation in Ultrasound Diffraction Tomography" with Prof. Sidney Leeman, University of London, Kings College, London, UK.

1.2 Training/Clinical Experience

- **Mammography Practicum**--Participated in a 1 week, 40 hour practicum for mammography technologists offered by the UCSD School of Medicine at the UCSD Medical Center. The course consisted of both lectures and working sessions and emphasized breast pathology, optimal mammography techniques and review and interpretation of mammograms with radiologists.

- **Clinical Trials**--Participated in the performance of clinical trials of patients at the UCSD Center for Women's Health designed to correlate conventional mammograms and sonography with ultrasound CT images. About twenty-five patients with a wide range of breast types and pathologies were studied. The work was carried out in close collaboration with mammography radiologists.

- **Diagnostic Imaging/Mammography Quality Control**--Participated in a wide-ranging number of diagnostic imaging equipment quality control surveys and radiation shielding planning and evaluation procedures. These activities are summarized in a table in Appendix 1. Of particular importance was participation in the **acceptance testing** of a GE Senographe DMR Mammography unit at the Veterans Affairs Medical Center, La Jolla, CA. in Dec. 1993 and the

subsequent submission of calibration and performance data to the ACR for **facility accreditation**. Accreditation was conferred on the first attempt in February, 1995.

- **Mammography Courses/Seminars**--Attended courses dealing with mammography quality control practices and regulations both at the AAPM Annual Meetings in Anaheim, CA in July, 1994 and in Philadelphia, PA in July, 1996 as well as at Southern California Chapter AAPM meeting in Carlsbad, CA, May, 1995.

- **AAPM Summer School**--Received 29 CEU units in Brachytherapy Physics by attending the 1994 AAPM Summer School at UCSD, San Diego, CA in June, 1994.

- **Mammography Quality Standards Act (MQSA)**--Intensive Practical Review offered by AAPM, 12 MPCEC units. Nov. 3-4, 1995, Pasadena, CA.

- **Breast Imaging and Interventions Course**--15 hours of CEU by the University of California at San Diego School of Medicine April 12-14, 1996 in breast imaging and interventions including diagnosis of breast pathology, quality standards and reporting, fine-needle core biopsies and ductography.

- **State of California Mammography Physicist**--Submitted application package to the State of California for registration as mammography physicist. Part of the application is a complete quality control survey of a mammography unit which was a GE DMR unit at the VA Medical Center in La Jolla, CA.

II. DISSERTATION RESEARCH

Tasks consistent with the Statement of Work of the fellowship proposal are briefly summarized. Example results are presented and some preliminary conclusions are drawn where appropriate. One task which was not called out directly in the proposal is the statistical evaluation of the raw data scattered by breast tissue. This follows recent work reported in the literature where such analyses are used to correct the transducer wavefront distortions in conventional B-scan ultrasound imaging. The application here, which extends the data to much lower frequencies than those reported before, is to use this analysis to characterize breast tissue and to obtain an *a priori* indicator of the degree of scattering and thus the validity of particular reconstruction algorithms. A second task which was added to the scope of the proposed Statement of Work is the evaluation of breast tissue contrast for some of the patients imaged as part of the clinical trials. This task was added when it became clear that some of the originally proposed system performance characterizations could not be completed due to problems with systems components that significantly reduced the availability of the SCT (Sonic Computed Tomography) breast imaging system.

A further expansion of the SOW is represented by the fact that during the reporting period a second transducer ring centered at 0.5 MHz was fabricated and integrated with the system. The motivation for adding such a low frequency ring arose out of the clinical trials which indicated

substantial attenuation and phase shifts for either large or very dense breasts. A lower frequency ring, though resulting in loss of resolution, was expected to have better signal to noise characteristics and thus provide improved images. Many of the tasks listed in the Statement of Work have been performed for both transducer rings.

2.1 Transducer Beam Pattern Characterization

One of the most fundamental system characterizations is the determination of the transducer radiation pattern and the effective slice width. The radiation pattern must be specified accurately for solution to the wave equation. For the sake of speed of calculation and mathematical simplicity, it is presently assumed to be represented by the first derivative of the Hankel function, that is, it is assumed to be dipole radiation with a $\cos\theta$ distribution. The extent to which the actual radiation (and receive) pattern deviates from such a distribution is of fundamental interest.

Measurements were carried out with the experimental geometry sketched in Figure 4. A needle hydrophone with approximately 0.03 in. diameter transducer element was positioned opposite an active transducer at roughly the center of the tank. The needle hydrophone was translated across the tank diameter and at each measurement position it was rotated to maximize signal, thus assuring that the position was radial. A second measurement series was carried out by recording the on-axis beam intensity as a function of distance from the transducer. This information is not only useful for mapping out the near to far-field transition but was used to correct the beam profile data to constant radial distance from the transducer. For the 0.5 MHz transducer ring, the needle hydrophone was found to be too insensitive to record the SCT (sonic computed tomography) transducer signals and a larger, 0.24 in. diameter transducer was employed.

Figure 5 is a polar plot of the radiation pattern for one of the transducers of the 1 MHz SCT ring. It is compared with both a $\cos\theta$ and a $(\cos\theta)^2$ distribution and is seen to fit somewhere in-between. The situation for the 0.5 MHz ring is depicted in Figure 6, which shows that, even with the coarseness of the data, the beam pattern is characterized by side-lobes that raise serious questions about the effect of the dipole-radiation assumption on the image reconstruction. The results for the lower frequency ring were anticipated since the lower length to width (L/D) ratio (due to greater detector width, 1.2 mm vs. .6 mm for the 1 MHz ring) results in a non-cylindrical antenna pattern.

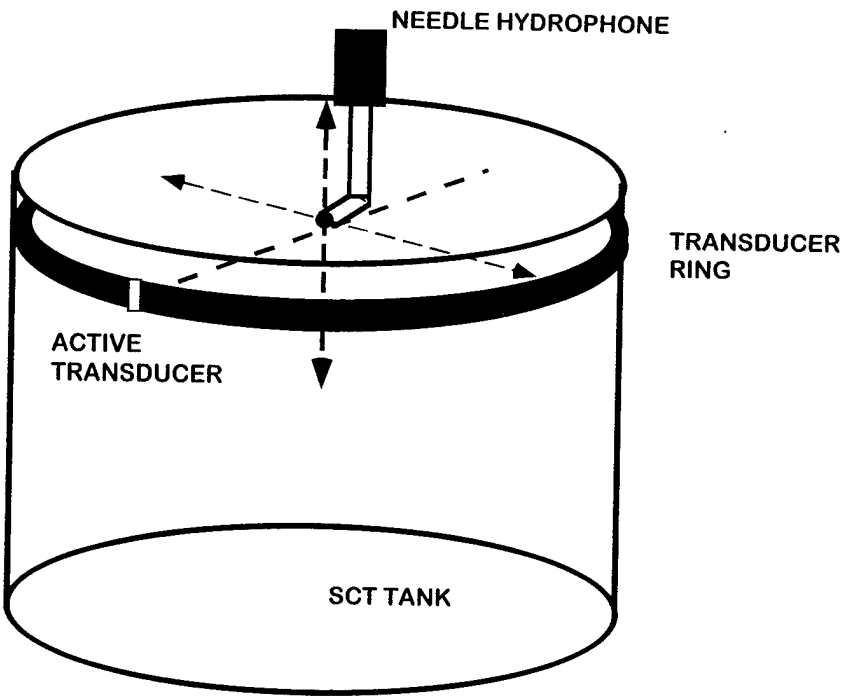

Figure 4. Schematic Diagram of SCT Transducer Beam Pattern and Slice Profile Determination using Needle Hydrophone

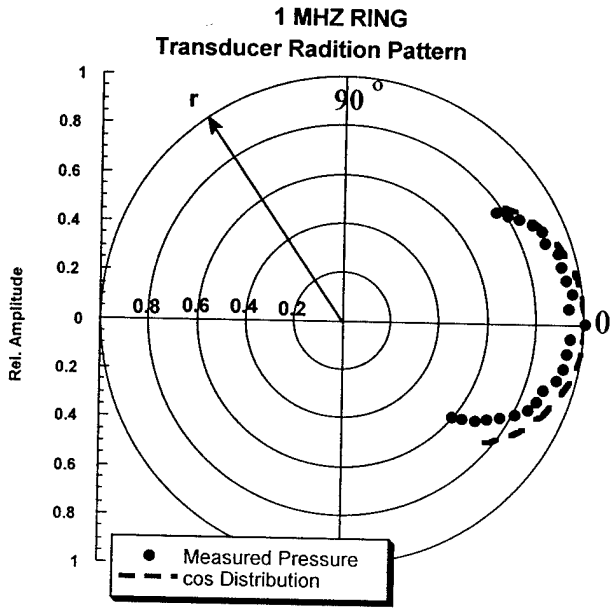

Figure 5. Polar Plot of Transducer Radiation Pattern. 1 MHz SCT Ring

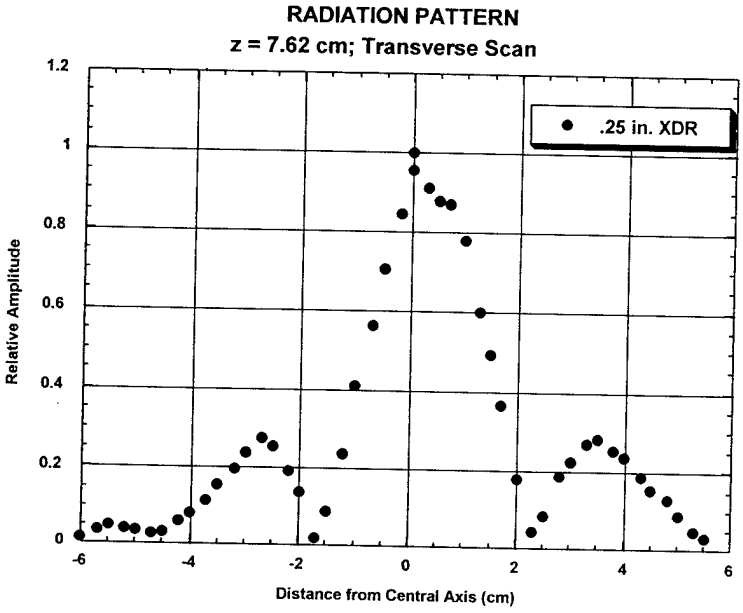

Figure 6. Radiation Pattern for 0.5MHz SCT Ring Showing Side Lobes.

2.2 Tomographic Slice Geometry

The measurement of effective slice geometry was performed at the center of the tank using the needle hydrophone for the 1 MHz ring and the 0.25 inch dia. transducer for the lower frequency ring. One transducer was excited and the axial pulse intensity distribution was measured by vertically translating the recording transducer. The results for the high frequency ring are displayed in Figure 7 and suggest that the slice width is essentially that of the transducer height (L), though the profile for the 0.5 MHz ring is not nearly as well defined as that for the higher frequency ring. It is to be noted that these data obtain only for one transducer at one location, the center of the tank.

What is also of interest is the effective slice width or sensitivity profile, measured as the axial range over which information shows up in the reconstructed image. Such a measurement was performed with two orthogonal nylon filaments inclined at approximately 45° angles. The filaments were 120 μm in diameter and were too small to be imaged with the 0.5 MHz SCT ring. With the 1 MHz ring, however, the resultant images were 1.1 and 1.2 cm, respectively, very much in agreement with the width of the profile in Figure 7.

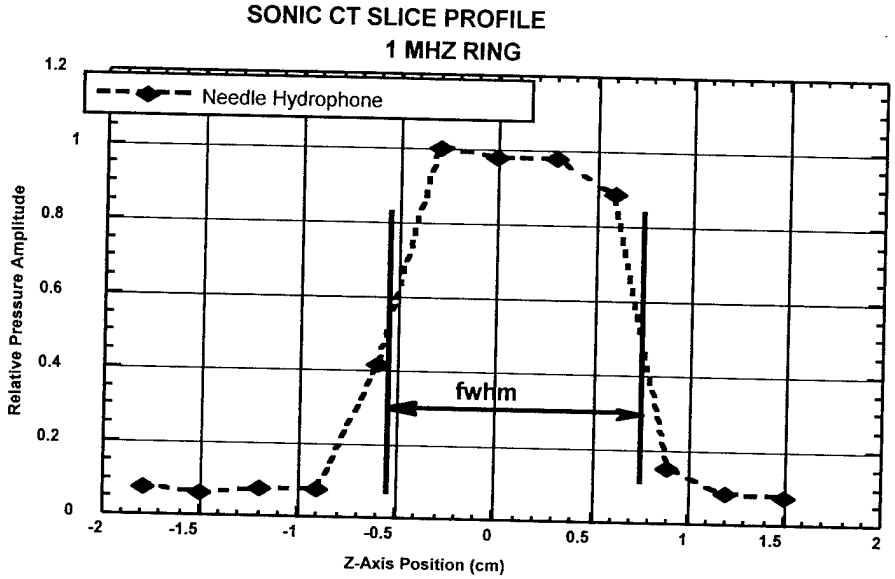

Figure 7. Slice Profile for 1 MHz SCT Ring

2.3 System MTF Measurements

A phantom incorporating 120 μm diameter nylon filaments arranged in rows with spacing between filaments ranging from 0.5 mm to 16 mm was constructed and used to measure the point-spread- function (PSF) at various locations within the measurement tank as well as at a number of discrete frequencies within the envelope of frequencies used for wide-band data acquisitions. These measurements were carried out with the 1 MHz SCT ring in water and thus represent the idealized system performance.

In general, if the 2-dimensional system point-spread function (the image of a point object or delta-function input) is given by PSF(x,y), then an object with true spatial characteristics o(x,y) will be blurred so that the image is represented by the convolution integral:

$$i(x,y) = \iint dx'\,dy'\,o(x',y')PSF(x-x',y-y') \tag{1}$$

which, by the convolution transform theorem is equivalent to the statement:

$$\tilde{I}(u,v) = \tilde{O}(u,v) * \tilde{H}(u,v) \tag{2}$$

where I, O and H are Fourier transforms of i, o and PSF in (1) with u,v the spatial frequency variables corresponding to x,y. The MTF is defined by the ratio of the blurred to the true object which is given by:

$$MTF = \frac{\left|\tilde{O}(u,v)\right|}{\left|\tilde{I}(u,v)\right|} = \left|\tilde{H}(u,v)\right| \tag{3}$$

The MTF was computed from measured point-spread functions due to the nylon filaments at several locations as well as for ten discrete frequencies ranging from 0.7 to 1.3 MHz. A typical result of such measurements is shown in Figure 8a which suggests that the cut-off frequency of the MTF is somewhere around 1 lp/mm which is roughly on the order of the theoretical limit for resolution of $\lambda/4$. We did not find much variation of the MTF with frequency, however, and this is a result that will be reviewed further. In particular, the PSF image is represented by very few points which makes the MTF calculation (using the FFT) less accurate. We will explore the feasibility of creating a speed of sound phantom with a sharply defined edge for which the line-spread-function (LSF) can be measured at some angle to provide more data points for the MTF calculation, a method commonly employed in x-ray CT.

The effect on the system resolution of the presence of an aberrating or scattering medium was initially explored by measuring the image of a nylon filament passing through balloons filled with solutions of various speeds of sound. Also shown in Figure 8b is the MTF for such a measurement and it can be seen that the cut-off frequency has been noticeably reduced from that for the filament in water. Thus, it is expected that the system MTF in more severely scattering or aberrating media such as agar and tissue-mimicking phantoms will be degraded even further. This topic will be revisited in experiments planned for the 0.5 MHz SCT ring as well in the near future.

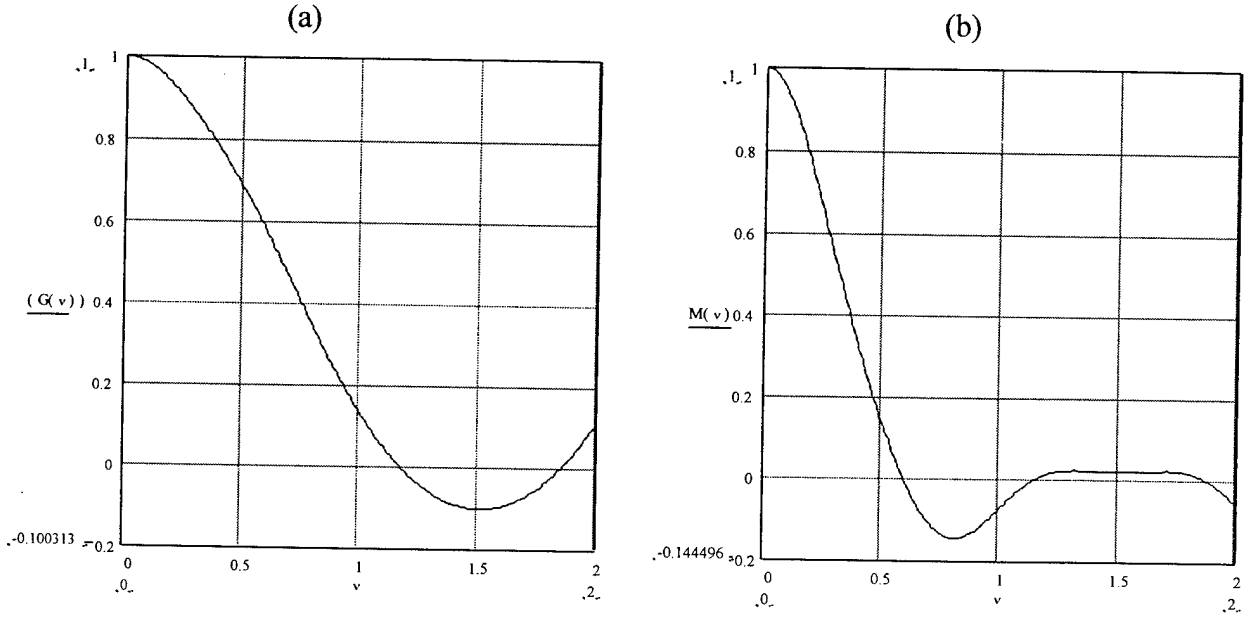

Figure 8. MTF of 1 MHz SCT Ring. First Order Born Magnitude Reconstruction. Object was 120 μm dia. Nylon Filament (a) in Water, (b) inside 2.75 in. dia. Balloon Filled with Saline Solution with Speed of Sound 4.7% Higher than Water.

2.4 Speed of Sound Contrast and Linearity

The solutions to the inverse scattering problem based on the Born approximation result in the reconstruction of the complex propagation constant:

$$k^2(x,y) = k_0^2(x,y)\left[n^2(x,y)+1\right] \qquad (4)$$

where $k_0 = \omega/c_0$; n, the refractive index, is given by: $n(x,y)=c(x,y)/c_0$ where c(x,y) is the speed of sound of the object and c_0 that of the medium. The real part of n reconstructs c(x,y), the imaginary part is an attenuation term (i.e. $n(x,y) = \alpha + i\beta$).

Measurements of the linearity of the reconstructed speed of sound over a range in speed from -11% to +9% relative to that of water were carried out with latex balloon phantoms filled with various ethanol (lower sound speed) and saline (higher sound speed) solutions. The balloons were nominally 3/4 in. in diameter thus representing scatterers of dimensions of several wavelengths at both nominal SCT ring frequencies of 0.5 and 1.0 MHz. Simulation calculations by GP Otto[1] had suggested non-linear behavior of the reconstructed sound speed and attenuation values for the various reconstruction algorithms currently employed. These are a beam-forming algorithm that results in a magnitude image (BFA) and two approaches to corrections to the first-order Born approximation (SM and STT algorithms) the discussion of which is beyond the scope of this summary report.

Measurements were conducted with both SCT rings by suspending four solution-filled balloons and obtaining an image. For each image, one of the balloons was filled water from the scanning tank as a reference. The reconstructed images were analyzed by recording the contrast (pixel values relative to that of the medium) of the images of the various solutions for both the real and imaginary images. An example of such an image pair is shown in Figure 9 which depicts the real (9a) and imaginary (9b) parts for low-to-medium contrast solutions and qualitatively satisfies the notion that higher sound speed should be bright and that the attenuation images should all appear similar since no significant differences in the attenuation values for the various solutions were expected.

Examples of speed of sound and attenuation contrast data for the 1 MHz SCT ring are provided in Figure 10. Similar results have been obtained recently with the 0.5 MHz ring using the same sound speed solutions. While conclusions are premature at this point, it appears that as the reconstruction algorithms become more sophisticated, incorporating time-of-flight and multiple scattering corrections, the linearity range of both speed of sound and attenuation appears to increase while contrast or sensitivity decreases. It should be noted that "attenuation" here does not refer to actual pressure amplitude or intensity reduction but simply the image pixel values for the imaginary part of the image plotted against phantom sound speed. We have already initiated experiments to measure similar data when the speed of sound objects are embedded in strongly aberrating media such as graphite-loaded agar and foam or breast-tissue mimicking materials that we have been experimenting with. The intent here, of course, is to see how the speed of sound contrast and linearity are affected when objects of dimensions on the order of several wavelengths are embedded in materials that significantly scatter and attenuate the incident wave.

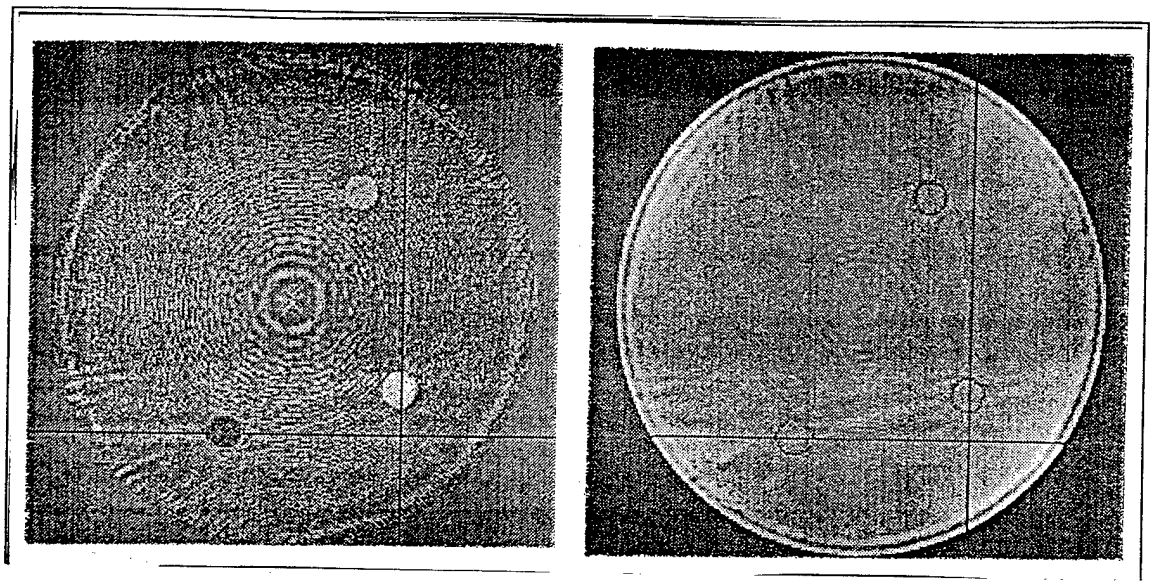

Figure 9. Real and Imaginary Components of Reconstructed Images of Medium Contrast Balloons using Beam Form Algorithm (TTC). Clockwise from top left: Water, 1.73% Saline, 1.89% Saline, -1.43% Ethanol.

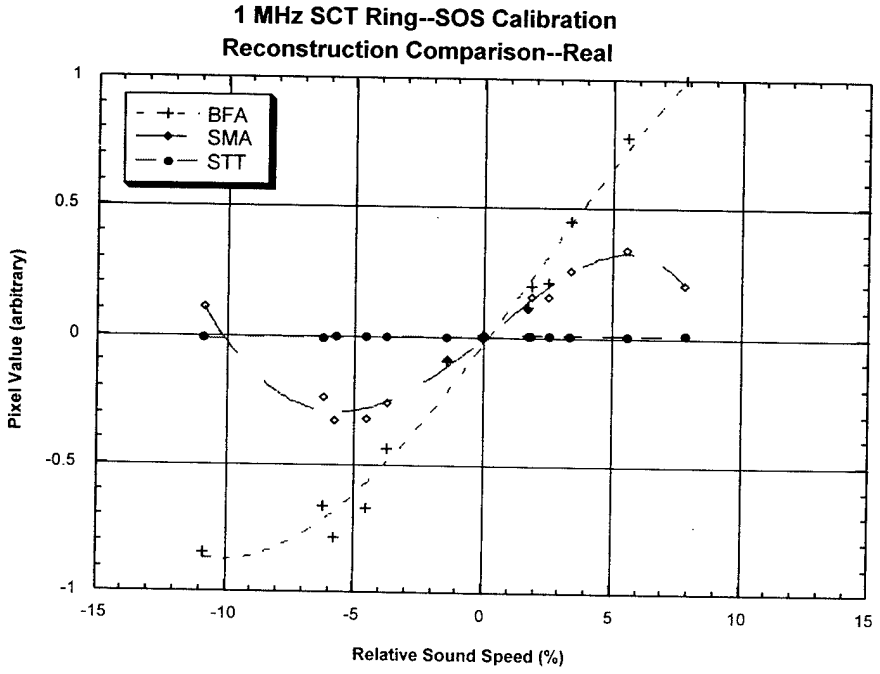

Figure 10 a. Speed of Sound Contrast Sensitivity for 1 MHz SCT Ring for Three Reconstruction Algorithms.

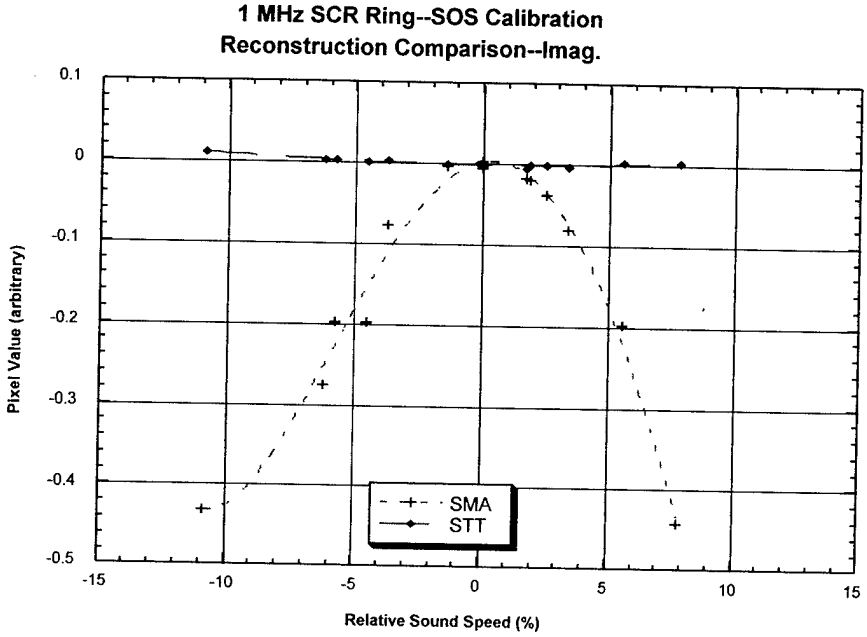

Figure 10 b. Attenuation Contrast Sensitivity for 1 MHz SCT Ring for Three Reconstruction Algorithms.

Examples of speed of sound and attenuation contrast data for the 1 MHz SCT ring are provided in Figure 10. Similar results have been obtained recently with the 0.5 MHz ring using the same sound speed solutions. While conclusions are premature at this point, it appears that as the reconstruction algorithms become more sophisticated, incorporating time-of-flight and multiple scattering corrections, the linearity range of both speed of sound and attenuation appears to increase while contrast or sensitivity decreases. It should be noted that "attenuation" here does not refer to actual pressure amplitude or intensity reduction but simply the image pixel values for the imaginary part of the image plotted against phantom sound speed. We have already initiated experiments to measure similar data when the speed of sound objects are embedded in strongly aberrating media such as graphite-loaded agar and foam or breast-tissue mimicking materials that we have been experimenting with. The intent here, of course, is to see how the speed of sound contrast and linearity are affected when objects of dimensions on the order of several wavelengths are embedded in materials that significantly scatter and attenuate the incident wave.

2.5 Scatter Amplitude Distribution Analysis

Wave propagation in the breast, according to a number of researchers,[26-32] is characterized principally by scatter and refraction and these processes are the primary causes of amplitude wavefront distortion. In the case of weak scattering, phase distortion can be

adequately addressed by various phase-aberration correction schemes. Amplitude distortion, however, is observed when scattering becomes strong and its appearance can be thought to define the limit of applicability of weak-scattering theories. In other words, scattering and refraction can be strong and thus one would not expect the first order Born approximation to hold since it implicitly assumes that scattering is weak. The evidence for this transition from weak to strong scattering is the shape of the observed probability density function (pdf) of the complex wavefront the modulus of which is approximated by a Rayleigh distribution. If scattering is weak, the observed distribution should be Rician and ultimately Gaussian.

Given that the reference waveform in the homogeneous medium at the receiver is:

$$E_o(x) = A_o(x)\exp(j\phi_o(x)) \tag{5}$$

and that with the object in the path:

$$E(x) = A(x)\exp(j\phi(x)) \tag{6}$$

the wavefront amplitude distortion term is defined as:

$$a(x) = A(x) / A_o(x) \tag{7}$$

By forming a histogram of the a(x) values, pdf vs. amplitude plots are obtained and compared to Rayleigh distributions of identical mean values. If there is close agreement between the two, that is if the standard deviations of the computed Rayleigh and the experimentally determined distributions are close, then the scatter field is considered to be fully developed.

The general form of the distribution to which our data were fitted is given by the expression:[36]

$$P(A) = \frac{A}{\sigma^2}\exp\left[-\frac{A^2 + A_0^2}{2\sigma^2}\right] I_0\left(\frac{AA_0}{\sigma^2}\right) \tag{8}$$

where P(A) is the probability density for amplitude A, A_0 has integral values and when $A_0 = 0$, (8) tends toward a Rayleigh distribution whereas for large values of A_0, P(A) becomes Gaussian. I_0 is the modified Bessel function. A more detailed development of the statistics of amplitude scattering is presented in Appendix 2.

We have extended this sort of analysis to lower frequencies by studying the scatter amplitude distributions from several patients who had been imaged as part of our clinical trials series at the UCSD Center for Women's Health. Patients had been imaged initially with the 1 MHz SCT ring and later on with the new low-frequency ring as well. One slice from each patient was analyzed according to the procedure outlined in Appendix 2. The initial analysis used only those receivers of the transducer ring that were in the shadow of the object. This is essentially comparable to the technique used by Steinberg and co-workers who used a single

transmitting transducer and a linear receiving array to record only pulses transmitted through the object. In our case we restricted the number of receiving transducers to the minimum value determined by an examination of the sinogram of the data. We are also analyzing scatter amplitude date from all receivers surrounding the object and will compare that with the sort of analysis exemplified in Figure 11.

It is observed that the index is lower for a breast that had had a lumpectomy with attendant radiation treatment than for a dense breast (patients 5 and 8, respectively) and also the index is lower for a fatty breast compared to a normal breast. Since these data are from only one coronal slice, it is not clear whether this ranking will hold when data from several tomographic slices of each breast are averaged. While the behavior with frequency for the low-frequency ring appears to be counter to expectations, the classifying index based on the mean value and standard deviation of the recorded amplitude distribution (i.e. $\mu = \langle x \rangle / \sigma$) appears to differentiate between breast tissue types.

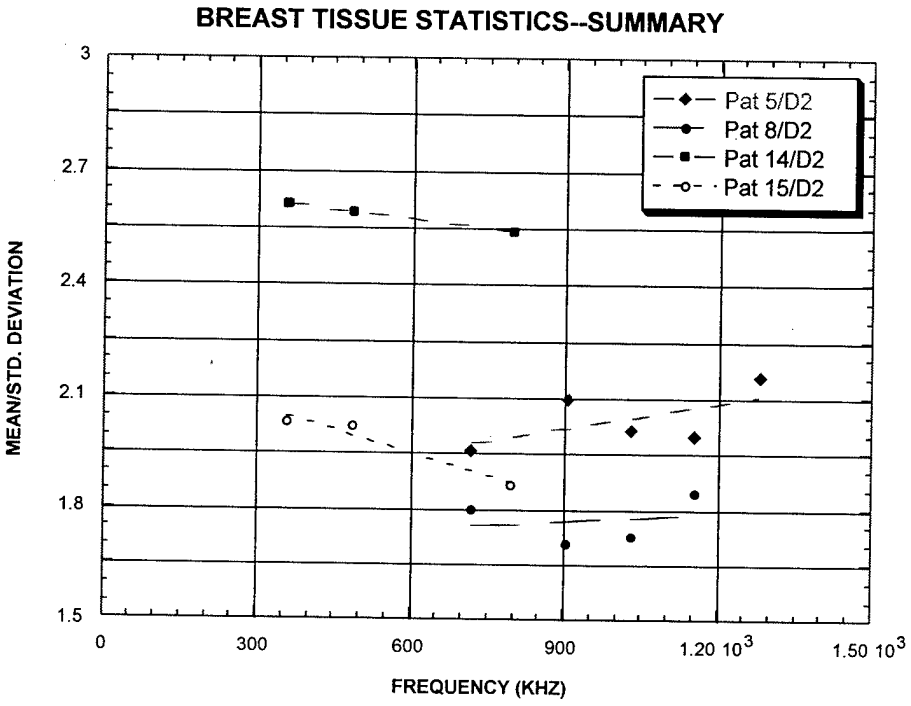

Figure 11. Scatter Distribution Index $\mu = \langle x \rangle / \sigma$ as a Function of Frequency for Four Patients with Breast Types: Pat. 5: Dense; Pat. 8: Fatty/Rad.Tx; Pat. 14:Normal; Pat. 15:Fatty

These analyses and further results are described in more detail in the paper of Appendix 3.

2.6 Tissue Contrast Determination

Ultrasound diffraction tomography is considered a quantitative imaging technique since there exists a direct, albeit complex, relationship between the nature of the scatter field (amplitude and phase) and the magnitude of the fluctuations in tissue properties such as compressibility, density and attenuation. In principle, such direct relationships hold for the case of exact solutions to the wave equation. It is not clear over what magnitude ranges in parameter fluctuations the images are quantitative when linearizing approximations are used to solve the wave equation and when noise, artifacts and aberrations are present. To make an initial empirical determination of the nature and magnitude range of image parameters, a number of patient images from our clinical trials were examined in detail in order to ascertain the following:

- Determination of tissue discrimination ability by checking values and consistency of image contrast of different tissue types within the breast and between patients.
- Determination of the uniformity of the pixel or gray scale value for key image features (e.g. water) within the breast, for different patients, the two transducer rings and various reconstruction algorithms.
- Determination of image presentations (real, imaginary, magnitude) and reconstructions (BFA, SMA, STT) which yield optimal tissue discrimination and consistency.

2.6.1. Approach

This is an initial attempt at establishing a procedure for analyzing images and as such it is subject to change and, hopefully, improvements. The evaluation procedures discussed here deal not with the raw, time-dependent data but with the reconstructed images and the pixel values of image elements of clinical significance. A radiologist (Dr. Ysrael in most instances) viewed images of coronal breast slices on the computer monitor and, with the aid of corresponding mammograms, identified the locations (x/y coordinates) and extents of significant tissue structures such as : **Skin, Subcutaneous Fat, Parenchyma, Ligaments, Cysts, Lesions** and **Unidentified Features.** Examples of the last item would be bright dots or specks that might represent calcifications or some unidentified strongly reflecting (or scattering) small object. Following this identification of key image features each was evaluated by recording mean pixel values for regions of interest (ROI's) that encompassed the feature. For each image slice, the mean pixel value for water was obtained by defining an annular region that excluded the breast object as well as artifact-filled regions adjacent to the transducer ring. The gray-scale value for water was used to compute the contrast for each image element from the relationship: $C = (p_{object} - p_{water})/|p_{water}|$. The use of the absolute value for the water pixel value assures that the sign of the contrast value unambiguously indicates the relationship to the pixel value of water which, very often, happens to be less than zero.

2.6.2. Preliminary Results

Image slices from eight patients (5,7,9,12,13,14,19 and 21) obtained with the two transducer rings were analyzed in this fashion. Since generally 10 or so tomographic slices are

available for each patient and since some were recorded with both SCT rings, even this preliminary data set is fairly large and time-consuming to produce. From a recording of the dimensions of the transducer ring, the pixel dimension is calculated and used to compute the sizes of objects or features identified by the radiologist. Thus, for the 1 MHz ring (Patients 5, 7, 9 and 12), pixel dimension are 0.21 x 0.21 mm and for the fifth slice of Patient 5, for example, the overall breast dimensions are 98.25 x 99.30 mm. Although the pixel value of the skin layer was recorded for many cases, it was found to range quite a bit and is not believed to be of diagnostic value. It is principally a function of the measurement geometry and may be an as yet poorly understood edge artifact.

a. Intra Breast Data

One of the important questions that was to be answered by this sort of review of the data is the consistency of image elements from slice to slice. Clearly, if the same feature or tissue type varies significantly in contrast from slice to slice, there is little hope of ever achieving general quantitative guidelines that will permit tissue identification on the basis of relative contrast level (i.e. scattering strength). In order to asses this, all slices for patients 5 , 7, 13 and 14 were analyzed and evaluated. The results are presented in the attached charts and some of the data are discussed briefly to provide insight into the nature of the contrast data.

Patient 5 is a dense, normal, right breast with diffuse calcifications. The plot of the raw pixel value data points reveals values much higher than for the other patients as well as some variation in the water value from slice to slice. The general trend is for the water values to decrease toward the chest wall and that may in part be due to the change in the area of the annular ring over which water values are averaged. The contrast values for parenchyma tissue are around 40% higher than water behind the nipple and then jump to around 100% above water in the middle of the breast. Subcutaneous fat generally is lower than water by as much as 50 %. These trends are reflected in the mean object contrast which is reasonably low for the first three slices but then jumps to values of 40 % or greater in the center of the breast. Figure 12 is a plot of percent tissue contrast for Patient 5 over the whole volume of the breast.

We observe in general that while differences between contrast values of different tissue types are fairly consistent throughout the breast volume, there appears to be a trend for all contrast values to increase toward the chest wall. It may be that this is somehow a result of the fact that the object dimensions increase toward the chest wall and thus the total attenuation through the object increases as well. Phantom studies will have to be carried out to determine the exact nature of this behavior.

The contrast values for subcutaneous fat are generally at or below the level of water suggesting that for medium-matching experiments one may wish to lower the water speed of sound with alcohol. However, how one changes the medium sound speed may well depend on what one wants to emphasize. Imaging the subcutaneous fat may be not nearly as important as imaging the glandular tissue and structures contained within it. Thus, one may want to use saline solutions to increase the medium speed of sound to more closely match the overall object value. Indeed, this is an interesting point for further investigation, for if one were to match the fat, penetration through that layer would be enhanced but then the overall contrast of the glandular tissue would even be higher and thus any advantage gained may be lost in the reconstruction.

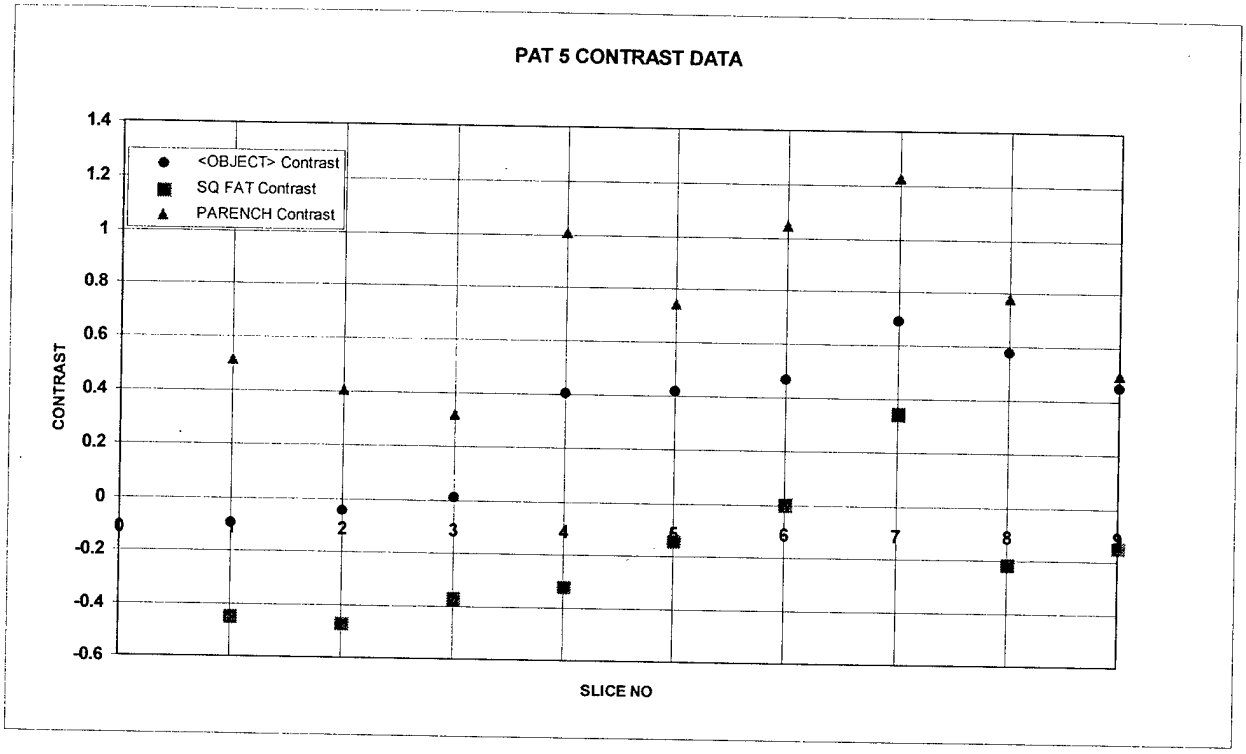

Figure 12. Percent Tissue Contrast for Normal Breast Tissue Elements for Patient 5.

All 0.5 MHz SCT ring images analyzed were first-order time-of-flight corrected images (BFC) and have real and imaginary components. The overall object contrast values for some of the patients are quite high, exceeding 100%. This in itself may be an indicator that the breast is either generally quite dense or contains significant elements of high density.

b. Inter-Breast Comparison

The relative consistency of breast tissue contrast within the breast is a critical requirement but also clearly desirable would be some rough correspondence between the same tissue type for different patients. To the extent that this was found to be the case for the patients and particular reconstructions evaluated is shown in Figure 13. Here are presented the magnitude tissue contrast values for five patients (5,7,9,12,13) and this comparison is of considerable interest.

The data in Figure 13 are for normal tissue components such as fat and parenchyma and two general observations can be made: The trend for contrast values to increase toward the chest wall is reflected in all cases and although the data exhibit considerable scatter, groupings by tissue type for all patients are quite clearly discernible. This suggests then, on the basis of very limited data, that the ultrasound diffraction images are, indeed, quantitative and able to distinguish between normal breast tissue types.

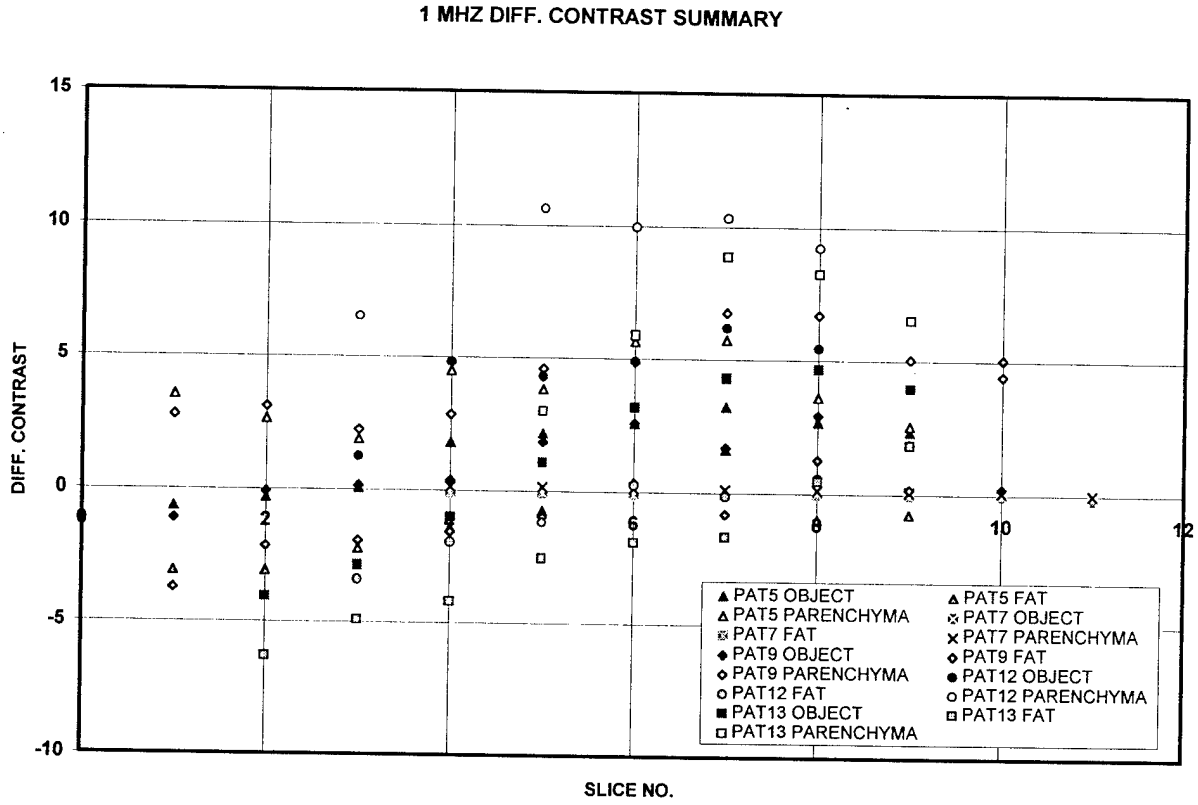

Figure 13. Summary of 1 Mhz SCT Data of Normal Breast Tissue Contrast for 5 Patients. Note that Parenchyma is open symbols, Fat shaded symbols and the mean Object contrast is represented by solid symbols.

A summary comparison of data from eight patients is afforded by Figure 14 which groups both normal and pathological tissue types whose values have been averaged over the whole breast volume. This data were obtained with both the 0.5 MHz and the 1 MHz SCT rings.

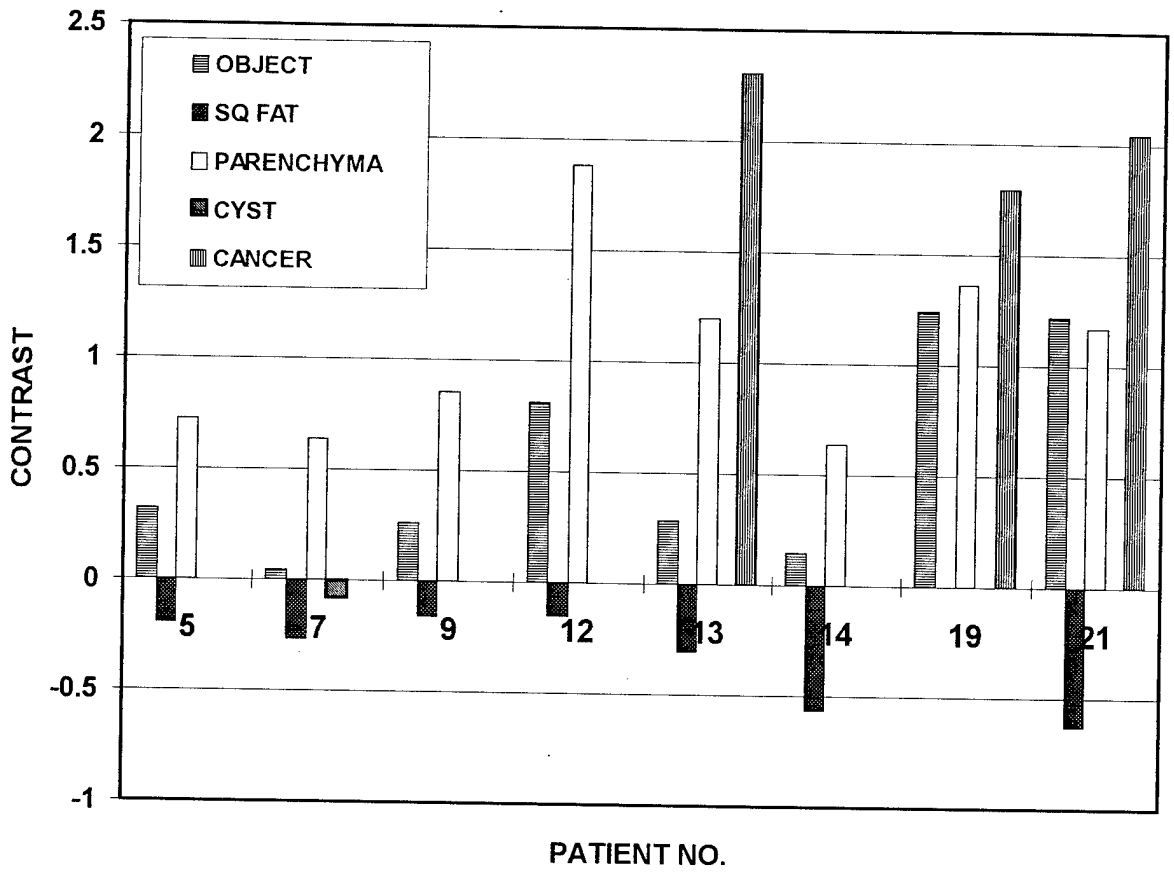

Figure 14. Summary of Mean Breast Tissue Contrast Values for Eight Patients Obtained with Two Transducer Rings (0.5 MHz and 1 MHz).

b1. Object Contrast

The overall object contrast is seen to vary quite a bit and is surprisingly low for Patient 7, something that a cursory evaluation of the images would not suggest. It is to be noted that the values presented here are means for all slices and these can fluctuate quite a bit depending on the distribution of fat vs. parenchyma, for example. As we saw in the previous section, there appears to be a tendency for the contrast values of most breast tissue components to be highest toward the center of the breast.

With the possible exception of Patient 7, the overall object contrast values are so high that serious concerns about the applicability of the Born Approximation have to be raised. With such high speed of sound variations and large object sizes total phase shifts with the 1 MHz ring can readily exceed 15 wavelengths and would be half that for the lower frequency ring. Since these are magnitude images it is difficult to determine what component of contrast is due to speed of

speed of sound and what is due to attenuation (we assume constant density since it is not explicitly contained in the wave equation). This suggests that the diffraction images are not explicitly speed of sound nor attenuation images but rather, images of fluctuations of the propagation constant, k. That is, k is a complex number whose real component is the speed of sound and whose imaginary component is the attenuation. With large objects or , more specifically, with large phase shifts, these components become mixed as a result of phase wrapping.

b2. Parenchyma

The contrast value for parenchyma is consistently high and quite consistent for the two rings. That it seems about twice as high with the .5 MHz ring as with the 1 MHz ring may well be a reflection of frequency and not due to significant tissue differences between patients. Such questions, of course, are most easily addressed by scanning the same breast with both rings, everything else being as equal as possible. We have attempted this with Patient 22/23 but system problems have prevented us from reaching any conclusions.

b3. Subcutaneous Fat

The tendency for subcutaneous fat to have lower contrast than water is consistent for all patients and again, we observe that the lower frequency transducer ring produces more than twice the contrast value observed at higher frequency.

b4. Cyst

Although only one data point exists so far (Patient 7), it is encouraging to note that the contrast value for a large fluid-filled cyst is close to that of water, something that was not apparent from a visual examination of the image. Additionally, septations suggested by ultrasound B-scan images were clearly identifiable in the diffraction image.

b5. Cancer

Contrast values for cancer appear quite high, somewhere between 30 and 60 percent above that of parenchyma. In addition to the higher numerical value, the appearance of parenchyma, when a large enough region of interest is selected, has distinct attributes that may be diagnostic.

2.7 Publications and Presentations

Some of the work of this fellowship was accepted for publication or presentation by the journals and conferences listed below.[37-49] This effort was in all cases the collaboration of several individuals and institutions and the opportunity to participate in these efforts is gratefully acknowledged.

- HS Janée, MP André, PJ Martin, GP Otto, BA Spivey, JP Jones, "Performance considerations of an ultrasound CT system for breast imaging", Medical Physics 21(6):1002, 1994.
- MP André, PJ Martin, HS Janée, GP Otto, BA Spivey, "Investigation of contrast sensitivity and phase aberration in low-frequency ultrasound diffraction tomography", Radiology 193(P):308, 1994.
- HS Janée, "Ultrasound tomography--a review of reconstruction techniques", presented at Colloquium in Radiological Sciences, University of California, Irvine, CA, (1994).
- GP Otto, MP André, PJ Martin, HS Janée, BA Spivey, "Frequency-dependent effects on image quality in a diffraction tomography system for breast imaging", J. Ultrasound Med 14 (3), 1995.
- HS Janée, JP Jones, MP André "Analysis of scatter fields in diffraction tomography experiments", Proceedings of 22nd International Symp. on Acoustical Imaging, Tortoli P. (ed.), Firenze, Italy: Consiglio Nazionale delle Ricerche, 1995.
- MP André, HS Janée, JP Jones, GP Otto, PJ Martin, "Reduction of phase aberration in a diffraction tomography system for breast imaging", Proceedings 22nd International Symp. on Acoustical Imaging, Tortoli P (ed.), Firenze, Italy: Consiglio Nazionale delle Ricerche, 1995.
- HS Janée, "Diagnostic Imaging / Mammography Certification and Quantitative Evaluation of Ultrasound CT Breast Imaging System", annual report to US Army Medical Research HQ, 1995.
- MP André, MZ Ysrael, LK Olson, HS Janée, RA Schulz, GP Otto, "Three-dimensional breast US: Holographic display of ultrasound CT", Radiology 197 (P), 1995.
- HS Janée, M.P. André, M.Z. Ysrael, L.K. Olson, G.R. Leopold, "Ultrasound Scatter Fields in the Breast: *In Vivo* Results with Diffraction Tomography",presented at 1996 AAPM Convention, Philadelphia, July 1996.
- MP André, HS Janée, GP Otto, PJ Martin, "Reduction of phase aberration in a diffraction tomography system for breast imaging", Acoustical Imaging 22, 1996. In Press.
- HS Janée, JP Jones, MP André, "Analysis of scatter fields in diffraction tomography experiments", Acoustical Imaging 22, 1996. In Press.
- MP André, HS Janée, GP Otto, PJ Martin, "Diffraction tomography with large-scale toroidal arrays", Int. J. Imaging Systems Technol., 1966. In Press.
- GP Otto, MP André, PJ Martin, HS Janée, BA Spivey, "Frequency-dependent effects on image quality in a diffraction tomography system for breast imaging", Amer. Inst. Ultrasound in Med., San Francisco, CA, March 1995.

CONCLUSIONS

Although this is the final report of the pre-doctoral fellowship, the research initiated within this program is ongoing and many conclusions are, perforce, preliminary. This is not a surprising situation for a new research area that explores a unique approach to breast imaging and requires not only new interpretations of images but an adaptation to a new presentation format. Some aspects of the fellowship grant, in particular those dealing with training and certification, require no conclusions other than the statement that certain objectives were realized and others are left to be accomplished.

I. Certification in Diagnostic Radiological Physics/Mammography

A considerable body of experience in diagnostic imaging equipment quality assurance and control has been obtained through course work at the University of California, Irvine and through surveys of many systems at a number of locations under the supervision of a board-certified medical physicist. Special efforts were made to prepare for certification in mammography with the State of California and an application for certification has been submitted. With the granting of the M.S. degree in Radiological Sciences, experience gained under the supervision of a certified physicist can be counted toward the work-experience requirements for eligibility to take the qualifying board examinations offered by the AAPM or ACR.

II. Dissertation Research

With the addition of the low-frequency transducer ring, many of the performance characterization tasks had to be carried out for both units. Thus, the Statement of Work has been expanded in scope if not in the nature of the tasks proposed. Ultimately the decision may be made to rely on only one of the transducer rings for general breast imaging. At this point, not enough information about the relative advantages and drawbacks of the two rings is available yet to formulate such a decision.

The measurements of transducer radiation patterns and tomographic slice profiles carried out so far suggest that the transducers of the 1 MHz SCT ring produce a radiation pattern that is a fair approximation to a dipole pattern. This cannot be said for the lower frequency ring the transducers of which have a lower L/D ratio and thus are characterized by a more complex radiation pattern. It will be one of the tasks for next year to investigate the effect of the deviation from a dipole pattern on the reconstructed images. It is to be noted here that the measurements so far have looked only at a few individual transducer elements and that it is assumed that the receive pattern of the transducers is similar to their transmit pattern. There are indications from the examination of the "noise image", that is the image of the water-filled tank, that these assumptions are largely valid.

The effective slice thickness has been found to be close to the long dimension of the transducers, an observation confirmed by examining the image of a nylon filament ramp obtained with the 1 MHz SCT ring. For clinical applications to breast imaging that slice width is undesirably wide and considerations are being given to perhaps a combination of hardware as well as data acquisition and processing procedural changes that might reduce the effective slice width of the image.

System MTF measurements to date have been only carried out for the higher frequency transducer ring and suggest that the cut-off frequency is in reasonable agreement with the theoretically expected resolution-limit. This, however, holds only for the ideal case for which a point-scatterer is suspended in the reference medium(water). The MTF becomes degraded when an object such as a cylinder filled with a somewhat different sound-speed solution is introduced and thus more serious deterioration is expected when a strongly scattering, large object like a breast is imaged. This effect will be explored in future experiments as will be the performance of the 0.5 MHz transducer ring. The investigation of the changes in MTF with transducer frequency so far has proven inconclusive. Some cyclical variations with frequency are observed that are not yet understood but may reflect a basic system operation/image reconstruction artifact.

Speed of sound contrast and linearity measurements have been carried out for both transducer rings but only the data for the 1 MHz ring have been analyzed so far. These measurements were for homogeneous, cylindrical objects that were several wavelengths in diameter and ranged in speed of sound relative to that of water from around -11% to +8%. The contrast of the reconstructed images when plotted against the refractive index or change in sound speed has linear ranges the widths of which (in terns of sound speed) depend on the reconstruction algorithm employed. The simplest, first-order Born approximation reconstruction yields the lowest linear range with, however, the highest sensitivity (defined as the change in image contrast with sound speed). More sophisticated reconstructions that employ time-of-flight corrections and attempts to treat multiple scattering appear to have wider linear ranges but markedly reduced sensitivity. It is premature to suggest that these are general conclusions and for the moment they only apply to a very narrow set of test objects and experimental conditions.

In a departure from the Statement of Work a task was added that examined the scattering process in breast tissue in some detail. A statistical analysis of the raw scattering data revealed that the amplitude distributions of these data appear to correlate with breast tissue type, though the exact nature of that correlation has not yet been established. If this trend holds reliably for many patients and breast types then it may be possible to design data acquisition and image reconstruction procedures that are optimized for each patient based on a quick statistical analysis of the scattered data from a "precursor" insonification of the tissue. In a preliminary analytical effort, an operator-based formalism has been developed that suggests that a range of linearizing approximations to the wave equation are possible and that the Born and Rytov approximations represent opposite endpoints to this range. Although the implementation of reconstructions based on such a general formalism are not obvious and beyond the scope of this work, the preliminary results of the statistical scatter analysis suggest that different breast images may be optimally reconstructed by a more Born-like or more Rytov-like approximation. This is an exciting development the difficulty of implementation of which cannot, however, be underestimated.

A second modification of the Statement of Work addresses the quantitative assessment of

tissue contrast for both normal breast tissue and pathologic tissue. Analogous to the Hounsfield scale used in x-ray computed tomography, tissue contrast is referenced to water and appears to be reliably differentiated by tissue type such as fat, parenchyma ligaments and vessels. A very encouraging preliminary finding is that benign structures such as fibrocysts and fibroadenomas and malignant lesions can be quantitatively differentiated from normal breast tissue. It is, however, critically important to stress that these findings are based on a very small sampling of the population and general conclusions must be deferred until a much larger and comprehensive data base is available.

REFERENCES

1. E. Silverberg and J. Lubera, Cancer Statistics, CA 37(e),1987.
2. J. Harris, M. Lippmann, U. Veronsesi et al, "Breast Cancer (Part 1), New England J. of Med. 327:319-328, 1992a.
3. A. Miller, E. Feuer, F. Hankey, "Recent incidence trends for breast cancer in women and relevance of early detection: An update", CA Cancer J. for Clinicians 43(1):27-41, 1993.
4. A. Miller, C. Baines, T. To, et al., "Canadian national breast screening study: 2. Breast cancer detection and death rates among women aged 50-59 years", Can. Med. Assoc. J. 147:1477-1488, 1992.
5. H. Collette, N. Day, J. Rombach, et al, "Evaluation of screening for breast cancer in a non-random study (the DOM project) by means of a case-control study", Lancet 1:1224-1226, 1984.
6. D. Kopans, "Years of study fail to quell breast screening controversy", Diag. Imag.:105-119, 1988.
7. "Essentials and Guidelines for Hospital Based Medical Physics Residency Training Programs", AAPM Report No. 36, Presidential Ad Hoc Committee on The Clinical Training of Radiological Physicists, 1990.
8. "Definition of a Qualified Medical Physicist in Mammography for ACR Mammography Accreditation Program", American College of Radiology Publication, 1993.
9. J. Meyer, M. Sonnenfeldt, R. Greenes, et al, "Preoperative localization of clinically occult breast lesions: Experience at a referral hospital", Radiology 169:627-628, 1988.
10. L. Baker, "Breast cancer detection demonstration project: Five year summary report", Cancer 32:194-225, 1982.
11. S. Hilton, G. Leopold, L. Olson, S. Wilson, "Real-time breast sonography: Application in 300 consecutive patients", AJR 147:479-486, 1986.
12. D. Kopans, J. Meyer, K. Lindfors, "Whole breast US imaging; four-year follow-up", Radiology 157:505-507, 1985.
13. E. Sickles, R. Filly, P. Callen, "Breast cancer detection with sonography and mammography", AJR 140:843-845, 1983.
14. B. Barraclough, J. Jellins, et al, "Breast ultrasound, the Australian perspective", *Ultrasonic Examination of the Breast,* J. Wiley and Sons, Chichester, 1983.
15. J. Greenleaf, S Johnson, W. Samayoa, F. Duck, "Algebraic reconstruction of spatial distributions of acoustic velocities in tissue from their time-of-flight profiles", *Acoustic Holography,* Plenum, New York, 1975.
16. G. Glover, J. Sharp, "Reconstruction of ultrasound propagation speed distributions in soft tissue: Time-of-flight tomography", IEEE Trans. Sonics Ultrasonics SU-24:229-234, 1977.
17. P. Carson, C. Meyer, A. Scherzinger, R. Oughton, "Breast imaging in coronal

planes with simultaneous pulse-echo and transmission ultrasound", Science 214:1141-1143, 1981.

18. M. Kaveh, R. Mueller, R. Rylander, T. Coulter, M. Soumekh, "Experimental results in ultrasonic diffraction tomography", Acoustical Imaging 9:433-450, 1979.
19. J. Greenleaf, J. Grisvold, R. Bahn, "A clinical prototype ultrasonic transmission tomographic scanner", Acoustic Imaging 12:579-587, 1982.
20. A. Yamada, K. Kurahashi, "Experimental image quality estimation of ultrasonic diffraction tomography", Jap. J. Appl. Phys. 32:2507-2509, 1993.
21. P. Martin, M. André, B. Spivey, D. Palmer, "Feasibility of a diffraction tomography technique which uses continuous-wave low-frequency ultrasound", submitted to Medical Physics.
22. P. Martin, M. André, B. Spivey, D. Palmer, G. Otto,"A new approach to computed tomography using low-frequency ultrasound", submitted to Radiology.
23. P. Martin, M. André, B. Spivey, D. Palmer, "Computed tomography using multi-hologram reconstruction of low-frequency ultrasound", presented at RSNA, 1992.
24. P. Martin, M. André, B. Spivey, D. Palmer, "Computed tomography for breast imaging", presented at Eighth Internat'l Congress on Ultrason. Exam. of the Breast, Heidelberg, Germany, 1993.
25. B. Spivey, P. Martin, D. Palmer, "Acoustic imaging device", U.S. Patent, 1995.
26. Q. Zhu and BD Steinberg, "Wavefront amplitude distribution in the female breast", J. Acoust. Soc. Am. 96(1):1-9, 1994.
27. Ibid, "Wavefront Amplitude Distortion and Image Sidelobe Levels: Part I--Theory and Computer Simulations" IEEE Trans. Ultrason. Ferroelect. Frequ. Control 40(6):747-753, 1993.
28. Ibid and RL Arenson, "Wavefront Amplitude Distortion and Image Sidelobe Levels: Part II--*In Vivo* Experiments", IEEE Trans. Ultrason. Ferroelect. Frequ. Control 40(6):754-762, 1993.
29. F. Stuart Foster and JW Hunt, "Transmission of Ultrasound Beams Through Human Tissue--Focussing and Attenuation Studies", Ultras. in Med. and Biol. 5:257-268, 1979.
30. M. Moshfeghi and RC Waag, "*In Vivo* and *In Vitro* Ultrasound Beam Distortion Measurements of a Large Aperture and a Conventional Aperture Focussed Transducer", Ultras. in Med. and Biol. 14(5):415-428, 1988.
31. GE Trahey, PD Freiburger, LF Nock, DC Sullivan, "*In vivo* measurements of ultrasonic beam distortion in the breast", Ultrason. Imag. 13:71-90, 1991.
32. Q. Zhu and BD Steinberg, "Large-transducer measurements of wavefront distortion in the female breast", Ultrason. Imag. 14:776-299, 1992.
33. PD Freiburger, DC Sullivan, BH LeBlanc, SW Smith, GE Trahey, "Two dimensional ultrasonic beam distortion in the breast: *in vivo* measurements and effects", Ultras. Imag. 14:398-414, 1992.
34. BD Steinberg, "A discussion of two wavefront aberration correction

procedures", Ultrason. Imag. 14:387-397, 1992.
35. M O'Donnell, SW Flax, "Phase aberration measurements in medical ultrasound: Human studies", Ultrason. Imag. 10:1-11, 1988.
36. A Ishimaru, Wave Propagation and Scattering in Random Media, Vol.1: Single Scattering and Transport Theory, Academic Press, NY 1978.
37. HS Janée, MP André, PJ Martin, GP Otto, BA Spivey, JP Jones, "Performance considerations of an ultrasound CT system for breast imaging", Medical Physics 21(6):1002, 1994.
38. MP André, PJ Martin, HS Janée, GP Otto, BA Spivey, "Investigation of contrast sensitivity and phase aberration in low-frequency ultrasound diffraction tomography", Radiology 193(P):308, 1994.
39. HS Janée, "Ultrasound tomography--a review of reconstruction techniques", presented at Colloquium in Radiological Sciences, University of California, Irvine, CA, (1994).
40. GP Otto, MP André, PJ Martin, HS Janée, BA Spivey, "Frequency-dependent effects on image quality in a diffraction tomography system for breast imaging", J. Ultrasound Med 14 (3), 1995.
41. HS Janée, JP Jones, MP André "Analysis of scatter fields in diffraction tomography experiments", Proceedings of 22nd International Symp. on Acoustical Imaging, Tortoli P. (ed.), Firenze, Italy: Consiglio Nazionale delle Ricerche, 1995.
42. MP André, HS Janée, JP Jones, GP Otto, PJ Martin, "Reduction of phase aberration in a diffraction tomography system for breast imaging", Proceedings 22nd International Symp. on Acoustical Imaging, Tortoli P (ed.), Firenze, Italy: Consiglio Nazionale delle Ricerche, 1995.
43. HS Janée, "Diagnostic Imaging / Mammography Certification and Quantitative Evaluation of Ultrasound CT Breast Imaging System", annual report to US Army Medical Research HQ, 1995.
44. MP André, MZ Ysrael, LK Olson, HS Janée, RA Schulz, GP Otto, "Three-dimensional breast US: Holographic display of ultrasound CT", Radiology 197 (P), 1995.
45. HS Janée, M.P. André, M.Z. Ysrael, L.K. Olson, G.R. Leopold, "Ultrasound Scatter Fields in the Breast: *In Vivo* Results with Diffraction Tomography", presented at 1996 AAPM Convention, Philadelphia, July 1996.
46. MP André, HS Janée, GP Otto, PJ Martin, "Reduction of phase aberration in a diffraction tomography system for breast imaging", Acoustical Imaging 22, 1996. In Press.
47. HS Janée, JP Jones, MP André, "Analysis of scatter fields in diffraction tomography experiments", Acoustical Imaging 22, 1996. In Press.
48. MP André, HS Janée, GP Otto, PJ Martin, "Diffraction tomography with large-scale toroidal arrays", Int. J. Imaging Systems Technol., 1966. In Press.
49. GP Otto, MP André, PJ Martin, HS Janée, BA Spivey, "Frequency-dependent effects on image quality in a diffraction tomography system for breast imaging", Amer. Inst. Ultrasound in Med., San Francisco, CA, March 1995.
50. J.W. Goodman, "Statistical Properties of Laser Speckle Patterns", Laser Speckle

and Related Phenomena, J.C. Dainty, Ed., pp.9-75, Springer Verlag, Heidelberg, 1975.

51. J.W. Goodman, Statistical Optics, John Wiley & Sons, New York, 1979.
52. J.W. Davenport, Jr., W.L. Root, Random Signals and Noise, McGraw-Hill, NY, 1958.
53. P. Beckmann, A. Spizzichino, The Scattering of Electromagnetic Waves from Rough Surfaces, Pergamon, Oxford, 1963.

APPENDIX 1

DIAGNOSTIC IMAGING QUALITY CONTROL EXPERIENCE SUMMARY

DATE	LOCATION	QC ACTIVITY
8-7-92	VAMC*	GE X-ray CT Unit Annual Survey
9-8-93	"	GE Senographe DMR Mammography Unit Acceptance Testing
6-23-94	Children's Hospital**	Mobile X-Ray Unit Annual Survey
7-23-94	"	Bi-Lateral Cardiology Unit (Toshiba) Acceptance Testing
10-8-94	"	Mobile X-Ray Units(5) Annual Survey
12-4-94	VAMC	Accreditation Testing, GE DMR Mammography Unit
12-15-94	"	Cardiac Cath Lab Radiation Shielding Evaluation
12-16-94	Children's Hospital	Radiography/Fluoroscopy Annual Surveys, Rooms 2,3 and 5
12-22-94	"	X-Ray CT Scanner, Room 4,5 Fluoroscopy Units Annual Survey
12-27-94	VAMC	GE DMR Mammography unit QC
1-2-95	Children's Hospital	OR C-Arm Unit, 2 Mobile C-Arm units, Mobile Dental Unit Annual QC
3-10-95	VAMC Outpatient Center***	Radiography/Fluoroscopy Suite Shielding Evaluation/Survey
5-10-95	VAMC	Room 3 Fluoroscopy Unit Annual QC
5-17-95	"	Room 1 Radiography Unit Annual QC
5-25-95	"	Room 1 Fluoroscopy Unit Annual QC
6-15-95	"	Room 7, Chest Unit Annual QC

6-26-95	"	**X-Ray CT Scanner Annual QC**
6-27-95	"	**Room 4, Cath. Lab Fluoroscopy Unit Annual CT**
1-7-96	"	**GE Senographe DMR Mammography Unit Annual Survey**

* Veterans Affairs Medical Center, La Jolla, CA.

** Sharpe/Children's Hospital, San Diego, CA

*** Veterans Affairs Medical Center Outpatient Clinic, San Diego, CA.

APPENDIX 2

SCATTER AMPLITUDE DISTRIBUTION ANALYSIS

A2.1 Statistics of the Complex Amplitude

When a wave such as an ultrasonic plane wave interacts with an object that is inhomogeneous and composed of an assembly of random scatterers, the resultant field is described by a complex scattering amplitude[50,51] :

$$A^{(r)} \equiv \mathrm{Re}\{A\} = \frac{1}{\sqrt{N}} \sum_{k=1}^{N} |a_k| \cos\phi_k$$
$$A^{(i)} \equiv \mathrm{Im}\{A\} = \frac{1}{\sqrt{N}} \sum_{k=1}^{N} |a_k| \sin\phi_k \qquad \text{(A2-1)}$$

It is to be noted that the average values of these amplitudes over a macroscopic ensemble is 0. The real and imaginary parts of the complex field thus have zero means, have identical variances and are uncorrelated.

If the number N is very large, i.e.if there are, as in our application, many scatterers, and the field thus is the sum of many independent random variables, then by the Central Limit Theorem[52,53], the amplitude distribution is Gaussian:

The pressure scatter field p is given by:

$$p = A\exp(i\phi) = X + iY \qquad \text{(A2-2)}$$

where A is the amplitude, ϕ the phase and X and Y are the sums of many independent contributions:

$$X = \sum_{i}^{N} X_i \qquad \text{and} \qquad Y = \sum_{i}^{N} Y_i \qquad \text{(A2-3)}$$

so that the field is the sum of:

$$p = \sum_{i}^{N} A_i \exp(i\phi_i) = \sum_{i}^{N} (X_i + iY_i) \qquad \text{(A2-4)}$$

The Central Limit Theorem says that the distributon of a random variable which is the sum of N independent random variables approaches normal as N becomes very large regardless of the distribution of each random variable. Thus X and Y are normally distributed if N is very large. Next, it is assumed that the phase ϕ_i is uniformly distributed over 2π since each component $A_i \exp(i\phi_i)$ is random and may be assumed to be uniformly distributed over 2π.

The probability density function of the amplitude A and the phase ϕ is then as follows:

$$P(A,\phi) = P(A)P(\phi), \qquad P(\phi) = 1/2\pi, \qquad 0 < \phi < 2\pi \tag{A2-5}$$

It can be easily shown that:

$$\langle X \rangle = \langle A\cos\phi \rangle = \int_0^{\infty} dA \int_0^{2\pi} d\phi A\cos\phi P(A,\phi) = 0$$

$$\langle Y \rangle = \langle A\sin\phi \rangle = 0$$

$$\langle XY \rangle = \langle A^2 \sin\phi\cos\phi \rangle = 0, \qquad \langle X^2 \rangle = \langle Y^2 \rangle = \sigma^2 = \int_0^{\infty} \pi A^2 P(A) dA \tag{A2-6}$$

It can be shown that, since X and Y are normally distributed:

$$P(X,Y) = P(X)P(Y) = \frac{1}{2\pi\sigma^2} \exp\left[-(X^2 + Y^2)/2\sigma^2\right] \tag{A2-7}$$

$$P(X,Y)dXdY = P(A,\phi)dAd\phi$$

Now $$dXdY = AdAd\phi, \qquad P(A) = \int_0^{2\pi} P(A,\phi)d\phi \tag{A2-8}$$

Then: $$P(A) = \frac{A}{\sigma^2}\exp(-A^2/2\sigma^2) \tag{A2-9}$$

This is the Rayleigh distribution which is characterized by a single parameter, the standard deviation. Thus the amplitude and phase of the scattered waves are independent, with the amplitude Rayleigh distributed and the phase uniformly distributed.

The development of the Rician or Rice-Nakagami[36] distribution follows along similar lines.

Let $\langle p \rangle = A_0 \exp(i\phi_0)$ be the coherent field. Letting the reference phase be 0, the incoherent field is given by $p_s = p - \langle p \rangle$ and is, as above, written as:

$$p_s = (X - A_0) + iY, \qquad X - A_0 = \sum_i^N X_i, \quad Y = \sum_i^N Y_i \tag{A2-10}$$

The probablity density function W(A), based on the Central limit theorem, is now given by:

$$W(X,Y) = \frac{1}{2\pi\sigma^2} \exp\left[-\frac{(X - A_0)^2 + Y^2}{2\sigma^2} \right] \tag{A2-11}$$

Then, by a similar argument to (A2-7 through A2-9), the probability density for the amplitude A is given by:

$$W(A) = \int_0^{2\pi} W(X,Y) A d\phi = \frac{A}{\sigma^2} \exp\left(-\frac{A^2 + A_0^2}{2\sigma^2}\right) I_0\left(\frac{A_0 A}{\sigma^2}\right) \tag{A2-12}$$

Where I_0 is the modified Bessel function. When the constant phasor $A_0 \rightarrow 0$, this reduces to the Rayleigh distribution in (A2-9). For large values of A_0 , W(A) becomes Gaussian. The ratio of the mean value of the distribution W(A) to its standard deviation is found to increase with A_0 and thus provides a useful index to indicate whether a scatterer is mostly Rayleighian or Rician. The Tissue Index is defined as : $TI = \bar{a} / \sigma_a$ and can be shown to be given[43] by:

$$\frac{\bar{a}}{\sigma_a} = \sqrt{\frac{\pi}{2}} \exp\left(-\frac{A_0^2}{4}\right) \left[\left(1 + \frac{A_0^2}{2}\right) I_0\left(\frac{A_0^2}{2}\right) + \frac{A_0^2}{2} I_1\left(\frac{A_0^2}{2}\right) \right] \tag{A2-13}$$

The ratio is unity for an exponential distribution, 1.24 for a Rayleigh distribution and becomes arbitrarily large with A_0 for a Rician distribution.

A2.2 Breast Tissue Scatter Amplitude

The wavefront amplitude distortion term defined in the Body section (equation 7) for our particular experimental geometry is given by:

$$a(x) = A(x) / A_w(x)$$

$$a_j = \tilde{A}_j^x / \tilde{A}_j^w \quad where \quad \langle \tilde{A}_j \rangle = \frac{1}{N-1} \sum_{k=1}^{N} \tilde{A}_{j,k} \ldots\ldots\ldots\ldots j \neq k \tag{A2-14}$$

where the index j refers to the receivers in the transducer ring and k to the transmitters. As defined, the amplitude ratio a_j for a particular receiver location is thus the mean of N-1 views of the object where N is either 1024 or 512.

The histogram data of the ratio of scattered pressure amplitude to that observed with the reference medium (water) are analyzed to see whether they are more nearly fit with a Rayleigh or Rician distribution. The Rayleigh distribution in scatter amplitude results when scattering and refraction are strong, suggesting that the object is composed of a large number of independent, random scatterers which produce uniform phase distributions and normal amplitude distributions. The modulus of such a distribution is Rayleighian. As scattering and refraction become weaker, the distribution tends toward a Rician distribution and ultimately toward a Gaussian.

A Tissue index was defined as : $m = \langle x \rangle / \sigma$ where $\langle x \rangle$ is the mean of the distribution and σ its standard deviation. This ratio is relatively low for a Rayleigh distribution and increases as the distribution tends toward Rician.

An example of a simple analysis using the Mathsoft Mathcad application is enclosed. The example is for a tomographic slice of the breast of Patient 15 which was classified by the mammography radiologist as dense. It is seen that the scatter amplitude distribution is best approximated by a Rician distribution with $k = 1$.

STATISTICAL EVALUATION OF SCATTER DATA FROM BREAST TISSUE
PATIENT 15 - 1.0 MHZ SCT RING

FILE: Pat15d2

a. Rayleigh Distribution Fit to Data

$m := 1..32$

$y_m := \frac{x_m}{1582}$ **Normalized Histogram**

Determination of Std. Deviation

$$x1 := \frac{\sum_{m=1}^{32} m \cdot x_m}{\sum_{m=1}^{32} x_m} \qquad x2 := \frac{\sum_{m=1}^{32} m^2 \cdot x_m}{\sum_{m=1}^{32} x_m}$$

$x1 = 7.612$

$x2 = 74.617$

$\sigma := \sqrt{x2 - x1^2}$

$\sigma = 4.084$

TISSUE INDEX:

$\frac{x1}{\sigma} = 1.864$

$$z_m := m \cdot \frac{\exp\left[-\frac{1}{2}\cdot\left(\frac{m}{\sigma}\right)^2\right]}{2.476}$$

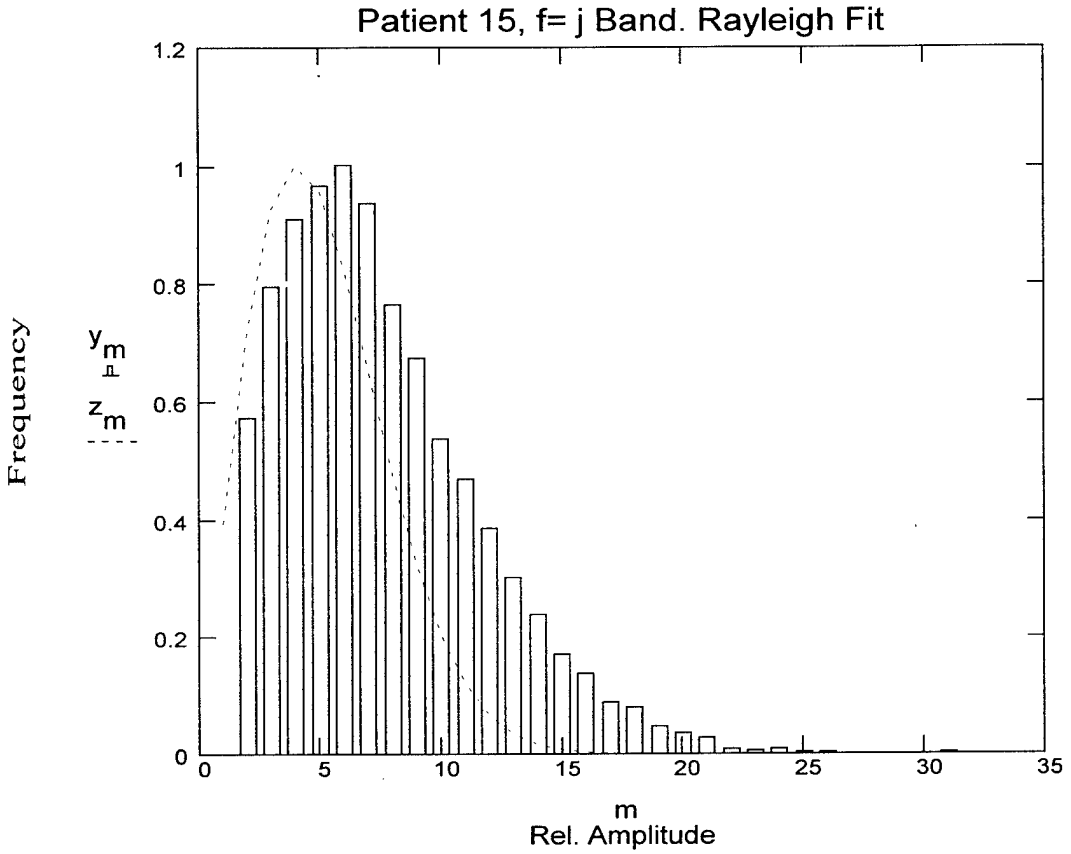

Figure 1. Scatter Amplitude Distribution for Patient 15, Slice 6 at nominally 0.70 MHz. Rayleigh Fit to Distribution. Std. Deviation calculated for normalized measured distribution. DISTRIB2 with banding and with (8:1) smoothing.

b. Rician Distribution

$k := 0..5$

$$s_{m,k} := m \cdot \exp\left[\frac{1}{2}\cdot\left(1+\left(\frac{m}{\sigma}\right)^2\right)-\frac{k^2}{2}\right]\cdot I0\left(k\cdot\frac{m}{\sigma}\right)$$

$$S_{m,0} := \frac{s_{m,0}}{2.476} \qquad S_{m,1} := \frac{s_{m,1}}{2.023} \qquad S_{m,2} := \frac{s_{m,2}}{1.731} \qquad S_{m,3} := \frac{s_{m,3}}{1.674}$$

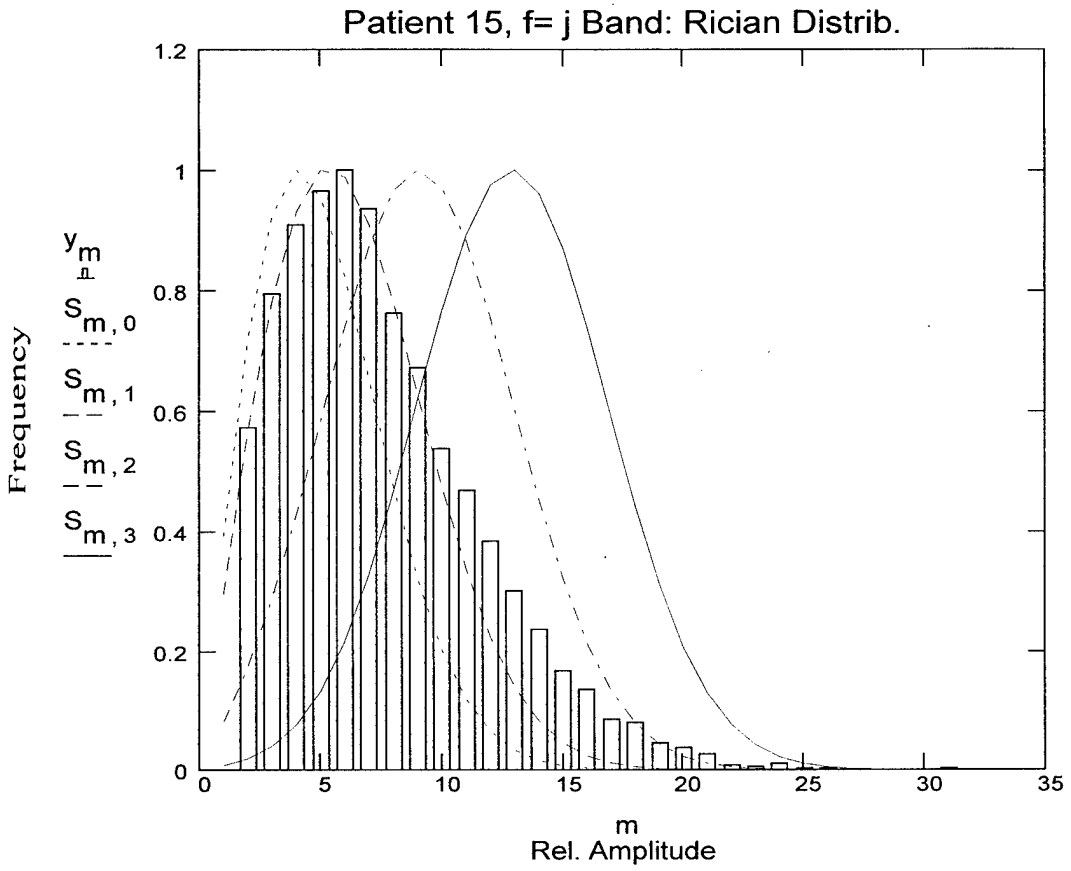

Figure 2. Rician Distributions Fit to Patient 15, Slice 6 Data from Figure 1. For Several values of k. k=0 tends toward Rayleigh Distribution. DISTRIB2.